CHAPTER 5

TWO-PHASE FLOW

TWO-phase flow is encountered extensively in the HVAC&R industries. A combination of liquid and vapor refrigerant exists in flooded coolers, direct-expansion coolers, thermosiphon coolers, brazed and gasketed plate evaporators and condensers, and tube-in-tube evaporators and condensers, as well as in air-cooled evaporators and condensers. In heating system pipes, steam and liquid water may both be present. Because the hydrodynamic and heat transfer aspects of two-phase flow are not as well understood as those of single-phase flow, no comprehensive model has yet been created to predict pressure drops or heat transfer rates. Instead, the correlations are for specific thermal and hydrodynamic operating conditions.

This chapter introduces two-phase flow and heat transfer processes of pure substances and refrigerant mixtures. Thus, some multiphase processes that are important to HVAC&R applications are not discussed here. The 2008 *ASHRAE Handbook—HVAC Systems and Equipment* provides information on several such applications, including humidification (Chapter 21), particulate contaminants (Chapter 28), cooling towers (Chapter 39), and evaporative air cooling (Chapter 40). See Chapter 41 of the 2006 *ASHRAE Handbook—Refrigeration* for information on absorption processes.

BOILING

Two-phase heat and mass transport are characterized by various flow and thermal regimes, whether vaporization occurs under natural convection or in forced flow. Unlike single-phase flow systems, the heat transfer coefficient for a two-phase mixture depends on the flow regime, thermodynamic and transport properties of both vapor and liquid, roughness of heating surface, wetting characteristics of the surface/liquid pair, and other parameters. Therefore, it is necessary to consider each flow and boiling regime separately to determine the heat transfer coefficient.

Accurate data defining regime limits and determining the effects of various parameters are not available. The accuracy of correlations in predicting the heat transfer coefficient for two-phase flow is generally not known beyond the range of the test data.

Boiling and Pool Boiling in Natural Convection Systems

Regimes of Boiling. The different regimes of pool boiling described by Farber and Scorah (1948) verified those suggested by Nukiyama (1934). The regimes are illustrated in Figure 1. When the temperature of the heating surface is near the fluid saturation temperature, heat is transferred by convection currents to the free surface, where evaporation occurs (region I). Transition to nucleate boiling occurs when the surface temperature exceeds saturation by a few degrees (region II).

In **nucleate boiling** (region III), a thin layer of superheated liquid forms adjacent to the heating surface. In this layer, bubbles nucleate and grow from spots on the surface. The thermal resistance of the superheated liquid film is greatly reduced by bubble-induced agitation and vaporization. Increased wall temperature increases bubble population, causing a large increase in heat flux.

As heat flux or temperature difference increases further and as more vapor forms, liquid flow toward the surface is interrupted, and a vapor blanket forms. This gives the **maximum heat flux**, which is

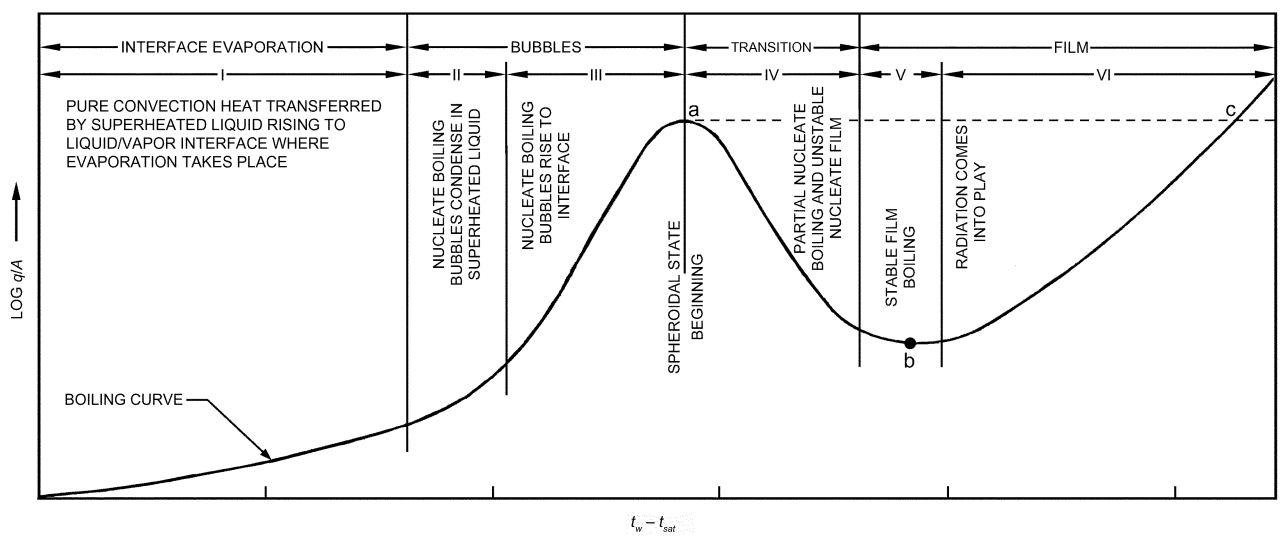

Fig. 1 Characteristic Pool Boiling Curve

The preparation of this chapter is assigned to TC 1.3, Heat Transfer and Fluid Flow.

at the **departure from nucleate boiling (DNB)** at point a in Figure 1. This flux is often called the **burnout heat flux** or **boiling crisis** because, for constant power-generating systems, an increase of heat flux beyond this point results in a jump of the heater temperature (to point c), often beyond the melting point of a metal heating surface.

In systems with controllable surface temperature, an increase beyond the temperature for DNB causes a decrease of heat flux density. This is the **transition boiling regime** (region IV); liquid alternately falls onto the surface and is repulsed by an explosive burst of vapor.

At sufficiently high surface temperatures, a stable vapor film forms at the heater surface; this is the **film boiling regime** (regions V and VI). Because heat transfer is by conduction (and some radiation) across the vapor film, the heater temperature is much higher than for comparable heat flux densities in the nucleate boiling regime. The **minimum film boiling (MFB)** heat flux (point b) is the lower end of the film boiling curve.

Free Surface Evaporation. In region I, where surface temperature exceeds liquid saturation temperature by less than a few degrees, no bubbles form. Evaporation occurs at the free surface by convection of superheated liquid from the heated surface. Correlations of heat transfer coefficients for this region are similar to those for fluids under ordinary natural convection [Equations (T1.1) to (T1.4)].

Nucleate Boiling. Much information is available on boiling heat transfer coefficients, but no universally reliable method is available for correlating the data. In the nucleate boiling regime, heat flux density is not a single valued function of the temperature but depends also on the nucleating characteristics of the surface, as illustrated by Figure 2 (Berenson 1962).

The equations proposed for correlating nucleate boiling data can be put in a form that relates heat transfer coefficient h to temperature difference $(t_s - t_{sat})$:

$$h = \text{constant}(t_s - t_{sat})^a \quad (1)$$

Exponent a is normally about 3 for a plain, smooth surface; its value depends on the thermodynamic and transport properties of the vapor and liquid. Nucleating characteristics of the surface, including the size distribution of surface cavities and wetting characteristics of the surface/liquid pair, affect the value of the multiplying constant and the value of a in Equation (1).

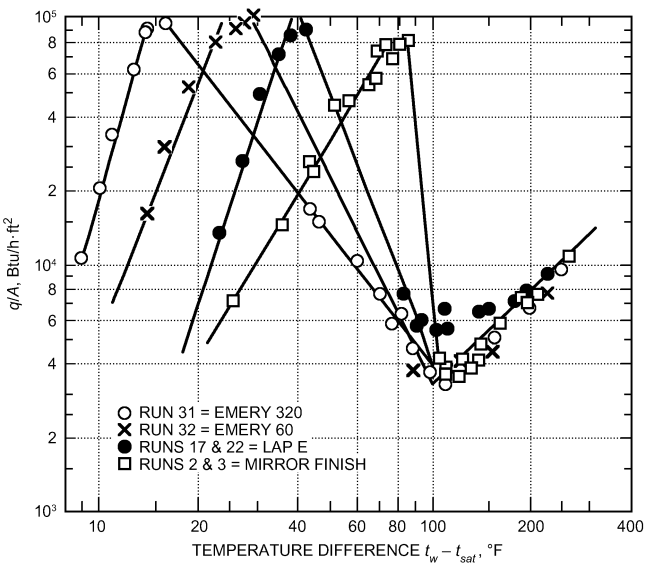

Fig. 2 Effect of Surface Roughness on Temperature in Pool Boiling of Pentane
(Berenson 1962)

A generalized correlation cannot be expected without considering the nucleating characteristics of the heating surface. Statistical analysis of data for 25 liquids by Hughmark (1962) shows that, in a correlation not considering surface condition, deviations of more than 100% are common.

In the following sections, correlations and nomographs for predicting nucleate and flow boiling of various refrigerants are given. For most cases, these correlations have been tested for refrigerants (e.g., R-11, R-12, R-113, and R-114) that are now identified as environmentally harmful and are no longer used in new equipment. Thermal and fluid characteristics of alternative refrigerants/refrigerant mixtures have recently been extensively researched, and some correlations have been suggested.

Stephan and Abdelsalam (1980) developed a statistical approach for estimating heat transfer during nucleate boiling. The correlation [Equation (T1.5)] should be used with a fixed contact angle θ regardless of the fluid. Cooper (1984) proposed a dimensional correlation for nucleate boiling [Equation (T1.6)]. The dimensions required are listed in Table 1. This correlation is recommended for fluids with poorly defined physical properties.

Gorenflo (1993) proposed a nucleate boiling correlation based on a set of reference conditions and a base heat transfer coefficient [Equation (T1.7)]. The correlation was developed for a reduced pressure p_r of 0.1 and the reference conditions given in Table 1. Base heat transfer coefficients are given for three fluids in Table 1; consult Gorenflo (1993) for additional fluids.

In addition to correlations dependent on thermodynamic and transport properties of the vapor and liquid, Borishansky et al. (1962), Lienhard and Schrock (1963) and Stephan (1992) documented a correlating method based on the law of corresponding states. The properties can be expressed in terms of fundamental molecular parameters, leading to scaling criteria based on reduced pressure $p_r = p/p_c$, where p_c is the critical thermodynamic pressure for the coolant. An example of this method of correlation is shown in Figure 3. Reference pressure p^* was chosen as $p^* = 0.029p_c$. This is a simple method for scaling the effect of pressure if data are available for one pressure level. It also is advantageous if the thermodynamic and particularly the transport properties used in several equations in Table 1 are not accurately known. In its present form, this correlation gives a value of $a = 2.33$ for the exponent in Equation (1) and consequently should apply for typical aged metal surfaces.

There are explicit heat transfer coefficient correlations based on the law of corresponding states for halogenated refrigerants (Danilova 1965), flooded evaporators (Starczewski 1965), and various other substances (Borishansky and Kosyrev 1966). Other investigations examined the effects of oil on boiling heat transfer from diverse configurations, including boiling from a flat plate (Stephan 1963), a 0.55 in. OD horizontal tube using an oil/R-12 mixture

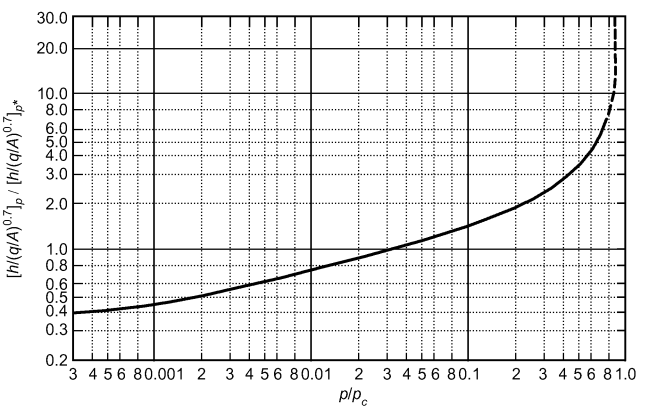

Fig. 3 Correlation of Pool Boiling Data in Terms of Reduced Pressure

Table 1 Equations for Boiling Heat Transfer

Description	References	Equations	
Free convection	Jakob (1949, 1957)	$\mathrm{Nu} = C(\mathrm{Gr})^m(\mathrm{Pr})^n$	(T1.1)
Free convection boiling, or boiling without bubbles for low Δt and $\mathrm{Gr\,Pr} < 10^8$. All properties based on liquid state.		Characteristic length scale for vertical surfaces is vertical height of plate or cylinder. For horizontal surfaces, $L_c = A_s/P$, where A_s is plate surface area and P is plate perimeter, is recommended. $\mathrm{Gr} = \frac{g\beta(t_s - t_{sat})L_c^3}{\nu^2}$	
Vertical submerged surface		$\mathrm{Nu} = 0.61(\mathrm{Gr})^{0.25}(\mathrm{Pr})^{0.25}$	(T1.2)
Horizontal submerged surface		$\mathrm{Nu} = 0.16(\mathrm{Gr})^{1/3}(\mathrm{Pr})^{1/3}$	(T1.3)
Simplified equation for water		$h \sim 80(\Delta t)^{1/3}$, where h is in Btu/h·ft²·°F, Δt in °F	(T1.4)
Nucleate boiling	Stephan and Abdelsalam (1980)	$\frac{hD_d}{k_l} = 0.0546\left[\left(\frac{\rho_v}{\rho_l}\right)^{0.5}\left(\frac{qD_d}{Ak_lt_{sat}}\right)\right]^{0.67}\left(\frac{h_{fg}D_d^2}{\alpha_l^2}\right)^{0.248}\left(\frac{\rho_l - \rho_v}{\rho_l}\right)^{-4.33}$	(T1.5)
		where $D_d = 0.0208\theta\left[\frac{\sigma}{g(\rho_l - \rho_v)}\right]^{0.5}$ with $\theta = 35°$.	
	Cooper (1984)	$h = 55p_r^{0.12-0.4343\ln(R_p)}(-0.4343\ln p_r)^{-0.55}M^{-0.5}\left(\frac{q}{A}\right)^{0.67}$	(T1.6)
		where h is in W/(m²·K), q/A is in W/m², and R_p is surface roughness in μm (if unknown, use 1 μm). Multiply h by 1.7 for copper surfaces.	
	Gorenflo (1993)	$h = h_oF_{PF}\left(\frac{q/A}{(q/A)_o}\right)^{nf}\left(\frac{R_p}{R_{po}}\right)^{0.133}$	(T1.7)
		where reference conditions for water are $(q/A)_o = 6300$ Btu/h·ft² and $R_{po} = 0.4$ μm	
		$F_{PF} = 1.2p_r^{0.27} + 2.5p_r + \frac{p_r}{1 - p_r}$	
		$nf = 0.9 - 0.3p_r^{0.15}$	
		For all fluids except water and helium.	
		Fluid — **h_o, Btu/h·ft²·°F**: R-134a 790; R-22 690; Ammonia 1230	
Critical heat flux	Kutateladze (1951)	$\frac{q/A}{\rho_v h_{fg}}\left[\frac{\rho_l^2}{\sigma g(\rho_l - \rho_v)}\right]^{0.25} = K_D$	(T1.8)
	Zuber et al. (1962)	For many liquids, K_D varies from 0.12 to 0.16; an average value of 0.13 is recommended.	
Minimum heat flux in film boiling from horizontal plate	Zuber (1959)	$\frac{q}{A} = 0.09\rho_v h_{fg}\left[\frac{\sigma g(\rho_l - \rho_v)}{(\rho_l + \rho_v)^2}\right]^{1/4}$	(T1.9)
Minimum heat flux in film boiling from horizontal cylinders	Lienhard and Wong (1964)	$q/A = 0.633\left\{\frac{4B^2}{1 + B/2}\right\}^{0.25}\left\{0.09\rho_v h_{fg}\left[\frac{g\sigma(\rho_l - \rho_v)}{(\rho_l + \rho_v)^2}\right]^{0.25}\right\}$	(T1.10)
		where $B = (2L_b/D)^2$ and $L_b = \left[\frac{\sigma}{g(\rho_l - \rho_v)}\right]^{0.5}$	
Minimum temperature difference for film boiling from horizontal plate	Berenson (1961)	$(t_s - t_{sat}) = 0.127L_b\left(\frac{\rho_v h_{fg}}{k_v}\right)\left[\frac{g(\rho_l - \rho_v)}{\rho_l + \rho_v}\right]^{2/3}\left[\frac{\mu_v}{g(\rho_l - \rho_v)}\right]^{1/3}$	(T1.11)
Film boiling from horizontal plate	Berenson (1961)	$h = 0.425\left[\frac{k_v^3\rho_v h_{fg}g(\rho_l - \rho_v)}{\mu_v(t_s - t_{sat})L_b}\right]^{0.25}$	(T1.12)
Film boiling from horizontal cylinders	Bromley (1950)	$h = 0.62\left[\frac{k_v^3\rho_v h_{fg}g(\rho_l - \rho_v)}{\mu_v(t_s - t_{sat})D}\right]^{0.25}$	(T1.13)
Effect of radiation	Anderson et al. (1966)	Substitute $h'_{fg} = h_{fg}\left(1 + 0.4c_p\frac{t_w - t_b}{h_{fg}}\right)$	
Quenching spheres	Frederking and Clark (1962)	$\mathrm{Nu} = 0.15(\mathrm{Ra})^{1/3}$ for $\mathrm{Ra} > 5 \times 10^7$	(T1.14)
		$\mathrm{Ra} = \left[\frac{D^3g(\rho_l - \rho_v)}{\nu_v^2\rho_v}\mathrm{Pr}_v\left(\frac{h_{fg}}{c_{p,v}(t_s - t_{sat})} + 0.4\right)\frac{a}{g}\right]^{1/3}$	
		where a = local acceleration	

(Tschernobyiski and Ratiani 1955), inside horizontal tubes using an oil/R-12 mixture (Breber et al. 1980; Green and Furse 1963; Worsoe-Schmidt 1959), and commercial copper tubing using R-11 and R-113 with oil content to 10% (Dougherty and Sauer 1974). Additionally, Furse (1965) examined R-11 and R-12 boiling over a flat horizontal copper surface.

Maximum Heat Flux and Film Boiling

Maximum, or critical, heat flux and the film boiling region are not as strongly affected by conditions of the heating surface as heat flux in the nucleate boiling region, making analysis of DNB and of film boiling more tractable.

Several mechanisms have been proposed for the onset of DNB [see Carey (1992) for a summary]. Each model is based on the scenario that a vapor blanket exists on portions of the heat transfer surface, greatly increasing thermal resistance. Zuber (1959) proposed that these blankets may result from Helmholtz instabilities in columns of vapor rising from the heated surface; another prominent theory supposes a macrolayer beneath the mushroom-shaped bubbles (Haramura and Katto 1983). In this case, DNB occurs when the liquid beneath the bubbles is consumed before the bubbles depart and allow surrounding liquid to re-wet the surface. Dhir and Liaw (1989) used a concept of bubble crowding proposed by Rohsenow and Griffith (1956) to produce a model that incorporates the effect of contact angle. Sefiane (2001) suggested that instabilities near the triple contact lines cause DNB. Fortunately, though significant disagreement remains about the mechanism of DNB, models using these differing conceptual approaches tend to lead to predictions within a factor of 2.

When DNB (point a in Figure 1) is assumed to be a hydrodynamic instability phenomenon, a simple relation [Equation (T1.8)] can be derived to predict this flux for pure, wetting liquids (Kutateladze 1951; Zuber et al. 1962). The dimensionless constant K varies from approximately 0.12 to 0.16 for a large variety of liquids. Kandlikar (2001) created a model for maximum heat flux explicitly incorporating the effects of contact angle and orientation. Equation (T1.8) compares favorably to Kandlikar's, and, because it is simpler, it is still recommended for general use. Carey (1992) provides correlations to calculate the maximum heat flux for a variety of geometries based on this equation. For orientations other than upward-facing, consult Brusstar and Merte (1997) and Howard and Mudawar (1999).

Van Stralen (1959) found that, for liquid mixtures, DNB is a function of concentration. As discussed by Stephan (1992), the maximum heat flux always lies between the values of the pure components. Unfortunately, the relationship of DNB to concentration is not simple, and several hypotheses [e.g., McGillis and Carey (1996); Reddy and Lienhard (1989); Van Stralen and Cole (1979)] have been put forward to explain the experimental data. For a more detailed overview of mixture boiling, refer to Thome and Shock (1984).

Hall and Mudawar (2000a, 2000b) presented an extensive review of critical heat flux data and correlations for flow boiling in tubes.

The minimum heat flux density (point b in Figure 1) in film boiling from a horizontal surface and a horizontal cylinder can be predicted by Equation (T1.9). The factor 0.09 was adjusted to fit experimental data; values predicted by the analysis were approximately 30% higher. The accuracy of Equation (T1.9) falls off rapidly with increasing p_r (Rohsenow et al. 1998). Berenson's (1961) Equations (T1.11) and (T1.12) predict the temperature difference at minimum heat flux and heat transfer coefficient for film boiling on a flat plate. The minimum heat flux for film boiling on a horizontal cylinder can be predicted by Equation (T1.10). As in Equation (T1.9), the factor 0.633 was adjusted to fit experimental data.

The heat transfer coefficient in film boiling from a horizontal surface can be predicted by Equation (T1.12), and from a horizontal cylinder by Equation (T1.13) (Bromley 1950).

Frederking and Clark (1962) found that, for turbulent film boiling, Equation (T1.14) agrees with data from experiments at reduced gravity (Jakob 1949, 1957; Kutateladze 1963; Rohsenow 1963; Westwater 1963).

Flooded Evaporators

Equations in Table 1 merely approximate heat transfer rates in flooded evaporators. One reason is that vapor entering the evaporator combined with vapor generated within the evaporator can produce significant forced convection effects superimposed on those caused by nucleation. Nonuniform distribution of two-phase, vapor/liquid flow in the tube bundle of shell-and-tube evaporators or tubes of vertical-tube flooded evaporators is also important.

Bundle data and design methods for plain, low-fin, and enhanced tubes were reviewed in Collier and Thome (1996) and Thome (1990).

Typical performance of vertical-tube natural circulation evaporators, based on data for water, is shown in Figure 4 (Perry 1950). Low coefficients are at low liquid levels because insufficient liquid covers the heating surface. The lower coefficient at high levels results from an adverse effect of hydrostatic head on temperature difference and circulation rate. Perry (1950) noted similar effects in horizontal shell-and-tube evaporators.

Forced-Convection Evaporation in Tubes

Flow Mechanics. When a mixture of liquid and vapor flows inside a tube, the flow pattern that develops depends on the mass fraction of liquid, fluid properties of each phase, and flow rate. In an evaporator tube, the mass fraction of liquid decreases along the circuit length, resulting in a series of changing vapor/liquid flow patterns. If the fluid enters as a subcooled liquid, the first indications of vapor generation are bubbles forming at the heated tube wall (nucleation). Subsequently, bubble, plug, churn (or semiannular), annular, spray annular, and mist flows can occur as vapor content increases for two-phase flows in horizontal tubes. Idealized flow patterns are illustrated in Figure 5A for a horizontal tube evaporator. Note that there is currently no general agreement on the names of two-phase flow patterns, and the same name may mean different patterns in vertical, horizontal and small tube flow. For detailed delineation of flow patterns, see Barnea and Taitel (1986) or Spedding and Spence (1993) for tubes and pipes between 0.125 and 3 in. in diameter, Coleman and Garimella (1999) for tubes less than 0.125 in. in diameter, and Thome (2001) for flow regime definitions useful in modeling heat transfer.

Increased computing power has allowed greater emphasis on flow-pattern-specific heat transfer and pressure drop models (although there is not uniform agreement among researchers and practitioners that this is always appropriate). Virtually all of the over 1000 articles on two-phase flow patterns and transitions have stud-

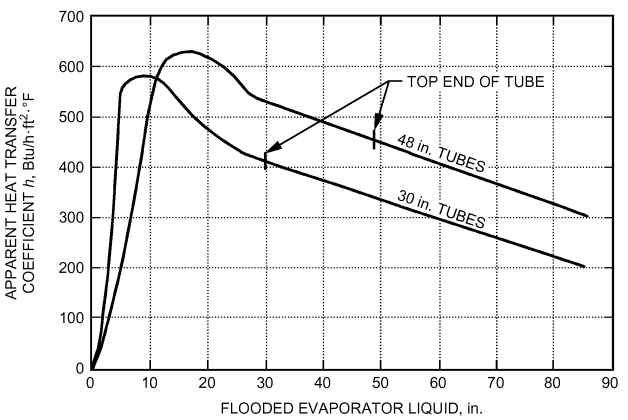

Fig. 4 Boiling Heat Transfer Coefficients for Flooded Evaporator
(Perry 1950)

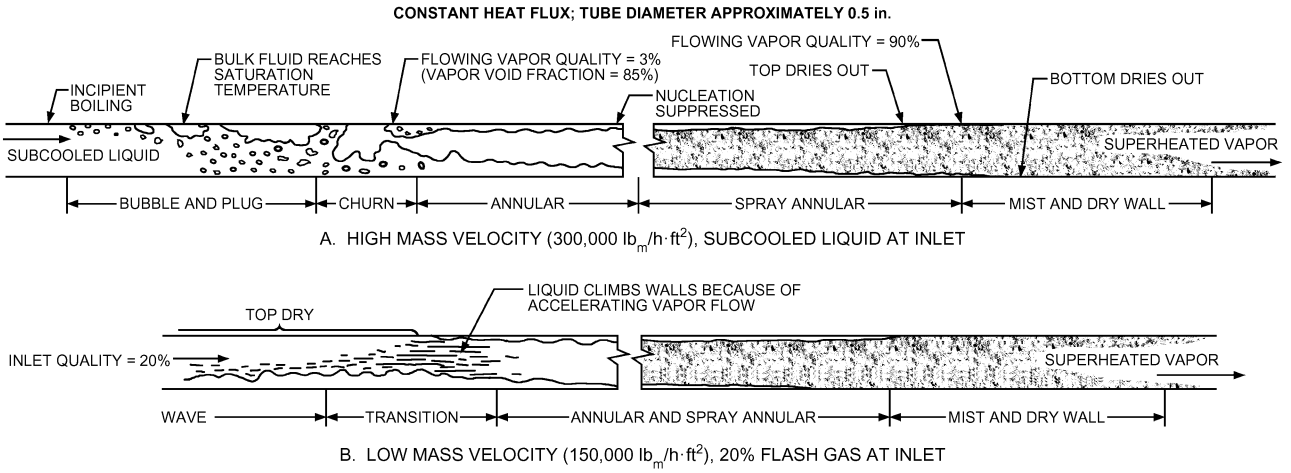

Fig. 5 Flow Regimes in Typical Smooth Horizontal Tube Evaporator

ied air/water or air/oil flows. Dobson and Chato (1998) found that the Mandhane et al. (1974) flow map, adjusted for the properties of refrigerants, produced satisfactory agreement with their observations in horizontal condensation. Thome (2003) summarized recent efforts to generate diabatic flow pattern maps in both evaporation and condensation for a number of refrigerants.

The concepts of vapor quality and void fraction are frequently used in two-phase flow models. **Vapor quality** x is the ratio of mass (or mass flow rate) of vapor to total mass (or mass flow rate) of the mixture. The usual flowing vapor quality or vapor fraction is referred to throughout this discussion. Static vapor quality is smaller because vapor in the core flows at a higher average velocity than liquid at the walls. In addition, it is very important to recognize that vapor quality as defined here is frequently not equal to the thermodynamic equilibrium quality, because of significant temperature and velocity gradients in a diabatic flowing vapor/liquid mixture. Some models use the thermodynamic equilibrium quality, and, as a result, require negative values in the subcooled boiling region and values greater than unity in the post-dryout or mist flow region. This is discussed further in Hetsroni (1986) and Kandlikar (1999).

The **area void fraction**, or just **void fraction**, ε_v is the ratio of the tube cross section filled with vapor to the total cross-sectional area. Vapor quality and area void fraction are related by definition:

$$\frac{x}{1-x} = \frac{\rho_v}{\rho_l} \times \frac{V_v}{V_l} \times \frac{\varepsilon_v}{1-\varepsilon_v} \tag{2}$$

The ratio of velocities V_v/V_l in Equation (2) is called the **slip ratio**. Note that the static void fraction and the flowing void fraction at a given vapor quality differ by a factor equal to the slip ratio.

Because nucleation occurs at the heated surface in a thin sublayer of superheated liquid, boiling in forced convection may begin while the bulk of the liquid is subcooled. Depending on the nature of the fluid and amount of subcooling, bubbles can either collapse or continue to grow and coalesce (Figure 5A), as Gouse and Coumou (1965) observed for R-113. Bergles and Rohsenow (1964) developed a method to determine the point of incipient surface boiling.

After nucleation begins, bubbles quickly agglomerate to form vapor plugs at the center of a vertical tube, or, as shown in Figure 5A, along the top surface of a horizontal tube. At the point where the bulk of the fluid reaches saturation temperature, which corresponds to local static pressure, there will be up to 1% vapor quality (and a negative thermodynamic equilibrium quality) because of the preceding surface boiling (Guerrieri and Talty 1956).

Further coalescence of vapor bubbles and plugs results in churn, or semiannular flow. If fluid velocity is high enough, a continuous vapor core surrounded by a liquid annulus at the tube wall soon forms. This occurs when the void fraction is approximately 85%; with common refrigerants, this equals a vapor quality of about 10 to 30%.

If two-phase mass velocity is high (greater than 150,000 $lb_m/h \cdot ft^2$ for a 0.5 in. tube), annular flow with small drops of entrained liquid in the vapor core (spray) can persist over a vapor quality range from about 10% to more than 90%. Refrigerant evaporators are fed from an expansion device at vapor qualities of approximately 20%, so that annular and spray annular flow predominates in most tube lengths. In a vertical tube, the liquid annulus is distributed uniformly over the periphery, but it is somewhat asymmetric in a horizontal tube (Figure 5A). As vapor quality reaches about 80% (the actual quality varies from about 70 to 90%, depending on tube diameter, mass velocity, refrigerant, and wall enhancement), portions of the surface dry out. Chaddock and Noerager (1966) found that, in a horizontal tube, dryout occurs first at the top of the tube and progresses toward the bottom with increasing vapor quality (Figure 5A). Kattan et al. (1998a, 1998b) indicated a very sharp decrease in the local heat transfer coefficient as well as the pressure drop at this point.

If two-phase mass velocity is low (less than 150,000 $lb_m/h \cdot ft^2$ for a 0.5 in. horizontal tube), liquid occupies only the lower cross section of the tube. This causes a wavy type of flow at vapor qualities above about 5%. As the vapor accelerates with increasing evaporation, the interface is disturbed sufficiently to develop annular flow (Figure 5B). Liquid slugging can be superimposed on the flow configurations illustrated; the liquid forms a continuous, or nearly continuous, sheet over the tube cross section, and the slugs move rapidly and at irregular intervals. Kattan et al. (1998a) presented a general method for predicting flow pattern transitions (i.e., a flow pattern map) based on observations for R-134a, R-125, R-502, R-402A, R-404A, R-407C, and ammonia.

Heat Transfer. It is difficult to develop a single relation to describe heat transfer performance for evaporation in a tube over the full quality range. For refrigerant evaporators with several percentage points of flash gas at entrance, it is less difficult because annular flow occurs in most of the tube length. However, the reported data are accurate only within the geometry, flow, and refrigerant conditions tested, so numerous methods for calculating heat transfer coefficients for evaporation in tubes are presented in Table 2 (also see Figure 6).

Figure 6 gives heat transfer data for R-22 evaporating in a 0.722 in. tube (Gouse and Coumou 1965). At low mass velocities (below 150,000 $lb_m/h \cdot ft^2$), the wavy flow regime shown in Figure 5B probably exists, and the heat transfer coefficient is nearly constant along the tube length, dropping at the exit as complete vapor-

Table 2 Equations for Forced Convection Evaporation in Tubes

Equations	Comments	References
$h = EE_2h_f + SS_2h_f$ (T2.1) where $E = 1 + 3000\ \mathrm{Bo}^{0.86}$ $S = 1.12\left[\frac{x}{(1-x)}\right]^{0.75}\left(\frac{\rho_l}{\rho_v}\right)^{0.41}$ $h_f = 0.023\ \mathrm{Re}_l^{0.8}\mathrm{Pr}_l^{0.4}(k_l/D)$ $\mathrm{Re}_l = \frac{G(1-x)D}{\mu_l}, \quad \mathrm{Bo} = \frac{q''}{Gh_{fg}}$ If tube is horizontal and Fr < 0.05, use the following multipliers: $E_2 = \mathrm{Fr}_l^{(0.1-2\ \mathrm{Fr}_l)} \qquad S_2 = \mathrm{Fr}_l^{1/2}$ $\mathrm{Fr}_l = \frac{G^2}{\rho_l g D}$ Otherwise, $E_2 = S_2 = 1$.	*Horizontal and Vertical* Compiled from a database of over 3600 data points, including data for R-11, R-12, R-22, R-113, R-114, and water. Useful for vertical flows and horizontal flows.	Gungor and Winterton (1987)
Boiling heat transfer coefficient h is the largest of that given by the following expressions: *Nucleate-boiling-dominated* (T2.2a) $\frac{h}{h_f} = 0.6683\left(\frac{\rho_l}{\rho_v}\right)^{0.1} x^{0.16}(1-x)^{0.64} f_2(\mathrm{Fr}_l) + 1058\,\mathrm{Bo}^{0.7}(1-x)^{0.8}F_{fl}$ *Convective-boiling-dominated* (T2.2b) $\frac{h}{h_f} = 1.136\left(\frac{\rho_l}{\rho_v}\right)^{0.45} x^{0.72}(1-x)^{0.08} f_2(\mathrm{Fr}_l) + 667.2\,\mathrm{Bo}^{0.7}(1-x)^{0.8}F_{fl}$ For $0.5 \le \mathrm{Pr}_l \le 2000$ and $10^4 \le \mathrm{Re}_l \le 5 \times 10^6$, $h_f = \frac{\mathrm{Re}_l\mathrm{Pr}_l(f/2)(k_l/D)}{1.07 + 12.7(\mathrm{Pr}_l^{2/3} - 1)(f/2)^{0.5}}$ For $0.5 \le \mathrm{Pr}_l \le 2000$ and $2300 \le \mathrm{Re}_l \le 10^4$, $h_f = \frac{(\mathrm{Re}_l - 1000)\mathrm{Pr}_l(f/2)(k_l/D)}{1 + 12.7(\mathrm{Pr}_l^{2/3} - 1)(f/2)^{0.5}}$ where $f = [1.58\ln(\mathrm{Re}_l) - 3.28]^{-2}$ For $\mathrm{Fr}_l < 0.04$ in horizontal tubes, $f_2(\mathrm{Fr}_l) = (25\ \mathrm{Fr}_l)^{0.3}$ For all other cases, $f_2 = 1$	*Horizontal and Vertical* Compiled from a database of 5246 data points, including data for R-11, R-12, R-22, R-113, R-114, R-152a, nitrogen, neon, and water. Tube sizes ranged from 0.25 to 1.25 in. Fluid-specific F_{fl} values are as follows (commercial copper tubes unless otherwise specified): Water 1.00 R-11 1.30 R-12 1.50 R-13B1 1.31 R-22 2.20 R-113 1.30 R-114 1.24 R-134a 1.63 R-152a 1.10 R-32/R-132 (60 to 40% wt.) 3.30 Kerosene 0.488 All fluids with stainless steel 1.0	Kandlikar (1999)
Boiling heat transfer coefficient h is the largest of that given by the following equations: $h = 230\ \mathrm{Bo}^{0.5}h_f$ (T2.3a) $h = 1.8\ [\mathrm{Co}(0.38\ \mathrm{Fr}_l^{-0.3})^n]^{-0.8}h_f$ (T2.3b) $h = F\exp\{2.47[\mathrm{Co}(0.38\ \mathrm{Fr}_l^{-0.3})^n]^{-0.15}\}h_f$ (T2.3c) $h = F\exp\{2.74[\mathrm{Co}(0.38\ \mathrm{Fr}_l^{-0.3})^n]^{-0.1}\}h_f$ (T2.3d) where h_f is calculated as for the Kandlikar correlation, and $F = 0.064\ \mathrm{Bo}^{0.5}$ if Bo > 0.0011 $F = 0.067\ \mathrm{Bo}^{0.5}$ if Bo < 0.0011 *Vertical*: $n = 0$ *Horizontal*: $n = 0$ if $\mathrm{Fr}_l > 0.04$ $n = 1$ for $\mathrm{Fr}_l < 0.04$ $\mathrm{Co} = \left(\frac{1-x}{x}\right)^{0.8}\left(\frac{\rho_v}{\rho_l}\right)^{0.5}$	*Horizontal and Vertical* Applicable to all fluids.	Shah (1982)

Table 2 Equations for Forced Convection Evaporation in Tubes (*Continued*)

Equations	Comments	References
$h = h_{mac} + h_{mic}$ where $h_{mac} = h_f E$ $h_{mic} = h_{pb} S$ $E = \left(1 + X_{tt}^{-0.5}\right)^{1.78} [(\mathrm{Pr}_l + 1)/2]^{0.444}$ $x_{tt} = \left(\frac{1-x}{x}\right)^{0.9} \left(\frac{\rho_v}{\rho_l}\right)^{0.5} \left(\frac{\mu_l}{\mu_v}\right)^{0.1}$ $S = 0.9622 - \tan^{-1}\left(\frac{\mathrm{Re}_l E^{1.25}}{6.18 \times 10^4}\right)$ $h_f = 0.023 \mathrm{Re}_l^{0.8} \mathrm{Pr}_l^{0.4} (k_l/D)$ $h_{pb} = \frac{0.00122 k_l^{0.79} c_{p,l}^{0.45} \rho_l^{0.49}}{\sigma^{0.5} \mu_l^{0.29} h_{fg}^{0.24} \rho_v^{0.24}} \Delta t_{sat}^{0.24} \Delta p_{sat}^{0.75}$ $\Delta t_{sat} = t_s - t_{sat}; \Delta p_{sat} = p_{sat}(t_s) - p_{sat}(t_{sat})$	(T2.4) *Vertical* This correlation is based on the idea that nucleation transfer mechanism h_{mic} and convective transfer mechanism h_{mac} are additive. Found to work well for low-pressure steam and some hydrocarbons.	Bennett and Chen (1980); Chen (1963)

Note: Except for dimensionless equations, units are lb_m, h, ft, °F, and Btu.

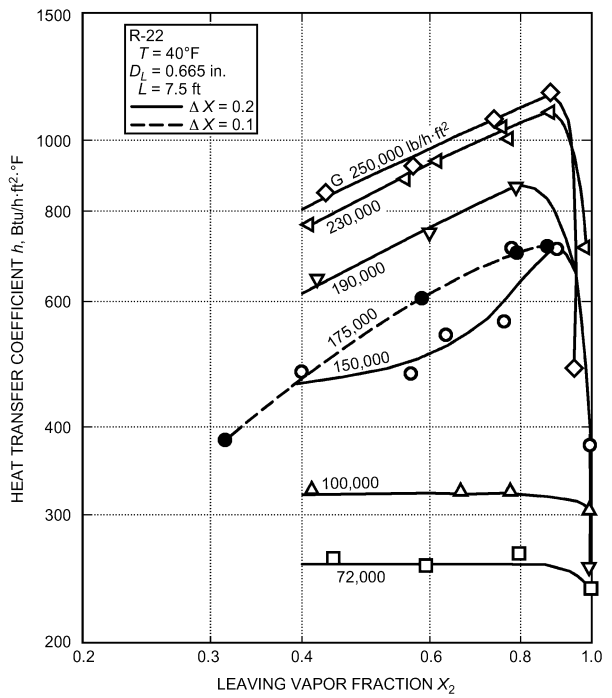

Fig. 6 Heat Transfer Coefficient Versus Vapor Fraction for Partial Evaporation

ization occurs. At higher mass velocities, flow is usually annular, and the coefficient increases as the vapor accelerates. As the surface dries and flow reaches between 70 and 90% vapor quality, the coefficient drops sharply.

Table 2 also gives methods to estimate local heat transfer coefficients during evaporation [e.g., Gungor and Winterton (1986); Kandlikar (1999)]. The Shah (1982) model [Equations (T2.3a) to (T2.3d)] is also recommended for estimating local heat transfer coefficients during annular flow. These local models have been found accurate for a wide range of refrigerants, but do not include ways to model dryout. The flow-pattern-based model described by Thome (2001) includes specific models for each flow pattern type and has been tested with newer refrigerants such as R-134a and R-407C.

Heat transfer coefficients during flow in vertical tubes can be estimated with the Chen (1963) correlation [Equation (T2.4)]. It includes terms for velocity effect (convection) and heat flux (nucleation) and produces local heat transfer coefficients as a function of local vapor quality. The Chen correlation is relatively simple and provides a good first estimate for vertical convective boiling, particularly for low-pressure steam. Although much more complex, the method developed by Steiner and Taborek (1992) includes an asymptotic model for the convection and nucleation component of heat transfer, and is recommended for most situations. This method requires fluid-specific constants, so is not presented in detail here; see Collier and Thome (1996) for more information.

The effect of lubricant on evaporation heat transfer coefficients has been studied by a number of authors. Eckels et al. (1994) and Schlager et al. (1987) showed that the average heat transfer coefficients during evaporation of R-22 and R-134a in smooth and enhanced tubes are decreased by the presence of lubricant (up to a 20% reduction at 5% lubricant concentration by mass). Slight enhancements at lubricant concentrations under 3% are observed with some refrigerant lubricant mixtures. Zeurcher et al. (1998) studied local heat transfer coefficients of refrigerant/lubricant mixtures in the dry wall region of the evaporator (see Figure 5) and proposed prediction methods. The effect of lubricant concentration on local heat transfer coefficients was shown to depend on mass flux and vapor quality. At low mass fluxes (less than about 150,000 $lb_m/h \cdot ft^2$), oil sharply decreased performance, whereas at higher mass fluxes (greater than 150,000 $lb_m/h \cdot ft^2$), enhancements at vapor qualities in the range of 0.35 to 0.7 were seen.

Boiling in Plate Heat Exchangers

For a description of plate heat exchanger geometry, see the Plate Heat Exchangers section of Chapter 4.

Little information is available on two-phase flow in plate exchangers; for brief discussions, see Hesselgreaves (1990), Jonsson (1985), Kumar (1984), Panchal (1985, 1990), Panchal and Hillis (1984), Panchal et al. (1983), Syed (1990), Thonon (1995), Thonon et al. (1995), and Young (1994).

General correlations for evaporators and condensers should be similar to those for circular and noncircular conduits, with specific constants or variables defining plate geometry. Correlations for flooded evaporators differ somewhat from those for a typical flooded shell-and-tube, where the bulk of heat transfer results mainly from pool boiling. Because of the narrow, complex passages in the PHE flooded evaporator, it is possible that the majority of heat transfer

occurs through convective boiling rather than localized nucleate boiling, which probably affects mainly the lower section of a plate in a flooded system. This aspect could be enhanced by modifying the surface structure of the lower third of the plates in contact with the refrigerant. It is also possible that the contact points (nodes) between two adjacent plates of opposite chevron enhance nucleate boiling. Each nodal contact point could create a favorable site for a re-entrant cavity.

The same applies to thermosiphon and direct-expansion evaporators. The simplest approach would be to formulate a correlation of the type proposed by Pierre (1964) for varying quality, as suggested by Baskin (1991). A positive feature about a PHE evaporator is that flow is vertical, against gravity, as opposed to horizontal flow in a shell-and-tube evaporator. Therefore, the flow regime does not get too complicated and phase separation is not a severe issue, even at low mass fluxes along the flow path, which has always been a problem in ammonia shell-and-tube direct-expansion (DX) evaporators. Generally, the profile is flat, except at the end plates. For more complete analysis, correlations could be developed that involve the local bubble point temperature concept for evaluation of wall superheat and local Froude number and boiling number Bo.

Yan and Lin's (1999) experimental study of a compact brazed exchanger (CBE) with R-134a as a refrigerant revealed some interesting features about flow evaporation in plate exchangers. Heat transfer coefficients were higher compared to circular tubes, especially at high-vapor-quality convective regimes. Mass flux played a significant role, whereas heat flux had very little effect on overall performance.

Ayub (2003) presented simple correlations based on design and field data collected over a decade on ammonia and R-22 direct-expansion and flooded evaporators in North America. The goal was to formulate equations that could be readily used by a design and field engineer without referral to complicated two-phase models. The correlations take into account the effect of chevron angle of the mating plates, making it a universal correlation applied to any chevron angle plate. The correlation has a statistical error of ±8%. The expression for heat transfer coefficient is

$$h = C(k_l/d_e)(\mathrm{Re}_l^2 h_{fg}/L_p)^{0.4124}(p_r)^{0.12}(65/\beta)^{0.35} \quad (3)$$

where $C = 0.1121$ for flooded and thermosiphons and $C = 0.0675$ for DX. This is a dimensional correlation where the values of k_l, d_e, h_{fg}, and L_p are in Btu/h·ft·°F, ft, Btu/lb, and ft, respectively. Chevron angle β is in degrees.

CONDENSING

In most applications, condensation is initiated by removing heat at a solid/vapor interface, either through the walls of the vessel containing the saturated vapor or through the solid surface of a cooling mechanism placed within the saturated vapor. If sufficient energy is removed, the local temperature of vapor near the interface drops below its equilibrium saturation temperature. Because heat removal creates a temperature gradient, with the lowest temperature near the interface, droplets most likely form at this location. This defines one type of heterogeneous nucleation that can result in either dropwise or film condensation, depending on the physical characteristics of the solid surface and the working fluid.

Dropwise condensation occurs on the cooling solid surface when its surface free energy is relatively low compared to that of the liquid. Examples include highly polished or fatty-acid-impregnated surfaces in contact with steam. **Film condensation** occurs when a cooling surface with relatively high surface free energy contacts a fluid with lower surface free energy [see Chen (2003) and Isrealachvili (1991)]; this type of condensation occurs in most systems.

For smooth film flow, the rate of heat transport depends on the condensate film thickness, which depends on the rates of vapor condensation and condensate removal. At high reduced pressures (p_r), heat transfer coefficients for dropwise condensation are higher than those for film condensation at the same surface loading. At low reduced pressures, the reverse is true. For example, there is a reduction of 6 to 1 in the dropwise condensation coefficient of steam when saturation pressure is decreased from 0.9 to 0.16 atm. One method for correlating the dropwise condensation heat transfer coefficient uses nondimensional parameters, including the effect of surface tension gradient, temperature difference, and fluid properties [see, e.g., Rose (1998)].

When condensation occurs on horizontal tubes and short vertical plates, condensate film motion is laminar. On vertical tubes and long vertical plates, film motion can become turbulent. Grober et al. (1961) suggest using a Reynolds number (Re) of 1600 as the critical point at which the flow pattern changes from laminar to turbulent. This Reynolds number is based on condensate flow rate divided by the breadth of the condensing surface. For the outside of a vertical tube, the breadth is the circumference of the tube; for the outside of a horizontal tube, the breadth is twice the length of the tube. $\mathrm{Re} = 4\Gamma/\mu_l$, where Γ is the mass flow of condensate per unit of breadth, and μ_l is the absolute (dynamic) viscosity of the condensate at film temperature t_f. In practice, condensation is usually laminar in shell-and-tube condensers with the vapor outside horizontal tubes.

Vapor velocity also affects the condensing coefficient. When this is small, condensate flows primarily by gravity and is resisted by the liquid's viscosity. When vapor velocity is high relative to the condensate film, there is appreciable drag at the vapor/liquid interface. The thickness of the condensate film, and hence the heat transfer coefficient, is affected. When vapor flow is upward, a retarding force is added to the viscous shear, increasing the film thickness. When vapor flow is downward, the film thickness decreases and the heat transfer coefficient increases. For condensation inside horizontal tubes, the force of the vapor velocity causes condensate flow. When vapor velocity is high, the transition from laminar to turbulent flow occurs at Reynolds numbers lower than 1600 (Grober et al. 1961).

When **superheated** vapor is condensed, the heat transfer coefficient depends on the surface temperature. When surface temperature is below saturation temperature, using the value of h for condensation of saturated vapor that incorporates the difference between the saturation and surface temperatures leads to insignificant error (McAdams 1954). If the surface temperature is above the saturation temperature, there is no condensation and the equations for gas convection apply.

Correlation equations for condensing heat transfer, along with their applicable geometries, fluid properties, and flow rates, are given in Table 3. The basic prediction method for laminar condensation on vertical surfaces is relatively unchanged from Nusselt's (1916). Empirical relations must be used for higher condensate flow rates, however.

For condensation on the outside surface of horizontal finned tubes, use Equation (T3.5) for liquids that drain readily from the surface (Beatty and Katz 1948). For condensing steam outside finned tubes, where liquid is retained in spaces between tubes, coefficients substantially lower than those given by this equation were reported, because of the high surface tension of water relative to other liquids. For additional data on condensation on the outside of finned tubes, please refer to Webb (1994).

Condensation on Inside Surface of Horizontal Tubes

A significant amount of work has been performed on internal flow condensation in recent years [see Cavallini et al. (2002) for a thorough overview]. Table 3 summarizes recommended correlations, along with the ranges of variables where the authors consider the correlations to be accurate. Note that the annular flow correlations assume uniform liquid film on the inside tube wall, which theoretically allows them to be applied to both vertical and horizontal

Table 3 Heat Transfer Coefficients for Film-Type Condensation

Description	References	Equations
Vertical Surfaces, Height *L*		
Laminar, non-wavy liquid film*	Based on Nusselt (1916)	$h = 0.943\left[\frac{\rho_l g(\rho_l-\rho_v)h_{fg}k_l}{\mu_l L^3(t_{sat}-t_s)}\right]^{1/4}$ (T3.1)
$\mathrm{Re} = 4\Gamma/\mu_l < 1800$		
$\Gamma = \dot{m}_l/b$ = mass flow rate of liquid condensate per unit breadth of surface		
Turbulent flow	McAdams (1954)	$h = 0.0077\left[\frac{k_l^3\rho_l(\rho_l-\rho_v)g}{\mu_l^2}\right]^{1/3}\mathrm{Re}^{0.4}$ (T3.2)
$\mathrm{Re} = 4\Gamma/\mu_f > 1800$		
Horizontal Tubes		
Single tube*	Dhir and Lienhard (1971)	$h = 0.729\left[\frac{k_l^3\rho_l(\rho_l-\rho_v)gh_{fg}}{\mu_l^2(t_{sat}-t_s)D}\right]^{1/4}$ (T3.3)
N tubes, vertically aligned	Incropera and DeWitt (2002)	$h = h_D N^{-1/4}$ (T3.4) where h_D is the heat transfer coefficient for one tube calculated from Dhir and Lienhard (1971).
Finned tubes	Beatty and Katz (1948)	$h = 0.689\left[\frac{\rho_l^2 k_l^3 g h_{fg}}{\mu_l(t_{sat}-t_s)D_e}\right]^{1/4}$ (T3.5)
This correlation is acceptable for low-surface-tension fluids and low-fin-density tubes. It overpredicts in cases where space between tubes floods with liquid (as when either surface tension becomes relatively large or fin spacing relatively small).		$\frac{1}{D_e^{1/4}} = 1.30\frac{A_s\phi}{A_{eff}L_{mf}^{1/4}} + \frac{A_p}{A_{eff}D^{1/4}}$
		$A_{eff} = A_s\phi + A_p$, $L_{mf} = \pi(D_o^2 - D_r^2)/D_o$
		ϕ = fin efficiency
		D_o = outside tube diameter (including fins)
		D_r = diameter at fin root (i.e., smooth tube outer diameter)
		A_s = fin surface area
		A_p = surface area of tube between fins
Internal Flow in Round Tubes		
Annular flow with uniform film distribution (horizontal or vertical)		
$0.002 < p_r < 0.44$,	Shah (1979)	$\mathrm{Nu} = \mathrm{Nu}_{lo}\left[(1-x)^{0.8} + \frac{3.8x^{0.76}(1-x)^{0.04}}{p_r^{0.38}}\right]$
$0 < x < 1$		$p_r = \frac{p}{p_c}$
$132.7\ \mathrm{lb/ft^2\cdot min} < G < 19{,}650\ \mathrm{lb/ft^2\cdot min}$		$\mathrm{Nu}_{lo} = 0.023\,\mathrm{Re}_l^{0.8}\mathrm{Pr}_l^{0.4}$ (T3.6)
$\mathrm{Re}_l > 350$		$\mathrm{Re}_l = \frac{GD}{\mu_l}$
$\mathrm{Pr}_l > 0.5$		
$10 < \rho_l/\rho_v < 2000$	Cavallini and Zecchin (1974)	$\mathrm{Nu} = 0.0344\,\mathrm{Re}_l^{0.83}\left[1 + x\left(\sqrt{\frac{\rho_l}{\rho_v}} - 1\right)\right]^{0.82}\mathrm{Pr}_l^{0.35}$ (T3.7)
$0.01 < \mu_v/\mu_l < 1$		
$5000 < \mathrm{Re} < 500{,}000$		
$\mathrm{Re} = \frac{GD}{\mu_l}$		
$0.8 < \mathrm{Pr}_l < 20$		
$0.1 < x < 0.9$		
	Fujii (1995)	$\mathrm{Nu} = 0.018\left(\mathrm{Re}_l\sqrt{\frac{\rho_l}{\rho_v}}\right)^{0.9}\left(\frac{x}{1-x}\right)^{(0.1x+0.8)}\mathrm{Pr}_l^{1/3}(1 + AH/\mathrm{Pr}_l)$ (T3.8)
		$H = \frac{c_{p,l}(t_{sat}-t_s)}{h_{fg}}$
		$A = 0.071\,\mathrm{Re}_l^{0.1}\left(\frac{\rho_l}{\rho_v}\right)^{0.55}\left(\frac{x}{1-x}\right)^{(0.2-1x)}\mathrm{Pr}_l^{1/3}$
Horizontal stratified wavy flow		
$G < 6144\ \mathrm{lb/ft^2\cdot min}$	Dobson and Chato (1998)	$\mathrm{Nu} = \mathrm{Nu}_{film} + \left(1 - \frac{\theta}{\pi}\right)\mathrm{Nu}_{forced}$ (T3.9)
$\mathrm{Fr}_m < 20$		$\left(1 - \frac{\theta}{\pi}\right) \approx \frac{\cos^{-1}(2\varepsilon_v - 1)}{\pi}$
		$\mathrm{Nu}_{film} = \frac{0.23\,\mathrm{Re}_v^{0.12}}{1 + 1.11X_{tt}^{0.58}}\left\{\frac{\mathrm{Ga}\,\mathrm{Pr}_l}{H}\right\}^{1/4}$ (*continued*)

Table 3 Heat Transfer Coefficients for Film-Type Condensation (*Continued*)

Description	References	Equations
		$\mathrm{Re}_v = \frac{GD}{\mu_v}$
$\mathrm{Fr}_m = a\left\{\frac{\mathrm{Re}_l^b}{\mathrm{Ga}^{0.5}}\right\}\left\{\frac{1+1.09X_{tt}^{0.039}}{X_{tt}}\right\}^{1.5}$		$H = \frac{c_{p,l}(t_{sat}-t_s)}{h_{fg}}$
$X_{tt} = \left(\frac{1-x}{x}\right)^{0.9}\left(\frac{\rho_v}{\rho_l}\right)^{0.5}\left(\frac{\mu_l}{\mu_v}\right)^{0.1}$		$\mathrm{Nu}_{forced} = 0.0195\,\mathrm{Re}_l^{0.8}\,\mathrm{Pr}_l^{0.4}\sqrt{1.376+\frac{a}{X_{tt}^b}}$
$\mathrm{Ga} = \frac{\rho_l(\rho_l-\rho_g)gD^3}{\mu_l^2}$		For $\mathrm{Fr}_t < 0.7$,
$a = 0.025$ and $b = 1.59$ if $\mathrm{Re}_l < 1250$		$a = 4.72 + 5.48\,\mathrm{Fr}_l - \mathrm{Fr}_l^2$
$a = 1.26$ and $b = 1.04$ if $\mathrm{Re}_l > 1250$		$b = 1.773 - 0.169\,\mathrm{Fr}_l$
		For $\mathrm{Fr}_t > 0.7$,
		$a = 7.242$, $b = 1.655$
		$\mathrm{Fr}_l = \frac{(G/\rho_l)^2}{gD}$

Note: Properties in Equation (T3.1) evaluated at $t_f = (t_{sat} + t_s)/2$; h_{fg} evaluated at t_{sat}. *For increased accuracy use $h'_{fg} = h_{fg} + 0.80c_{p,v}(t_{sat} - t_s)$ in place of h_{fg}.

flows. The Shah (1979) model has been verified for both orientations by several research groups; the Cavallini and Zecchin (1974) and Fujii (1995) models have been shown effective for horizontal flow.

Outside the annular flow regime, care must be taken to account for asymmetry in the liquid film in horizontal flow. The Dobson and Chato (1998) model adapts previous work and captures the effects of gravity fairly well. Condensation in vertical tubes becomes very complex if the vapor and liquid are in counterflow (i.e., vapor flows upward against gravity), although there are applications (e.g., reflux condensers) where this mode is an intentional part of the design. See Palen and Yang (2001) for more information on reflux condenser design.

As with convective evaporation, progress is being made in implementing flow-regime-based models for convective internal flow condensation. Models for flow regime transitions during condensation of pure components in a horizontal tube are presented in Breber et al. (1980) and El Hajal et al. (2003); Dobson and Chato (1998) and Thome et al. (2003) describe prediction methods for flow-regime-based heat transfer coefficients.

Noncondensable Gases

Condensation heat transfer rates reduce drastically if one or more noncondensable gases are present in the condensing vapor/gas mixture. In mixtures, the condensable component is called *vapor* and the noncondensable component is called *gas*. As the mass fraction of gas increases, the heat transfer coefficient decreases in an approximately linear manner. In a steam chest with 2.89% air by volume, Othmer (1929) found that the heat transfer coefficient dropped from about 2000 to about 600 Btu/h·ft²·°F.

Consider a surface cooled to temperature t_s below the saturation temperature of the vapor (Figure 7). In this system, accumulated condensate falls or is driven across the condenser surface. At a finite heat transfer rate, the temperature profile across the condensate can be estimated from Table 3; the interface of the condensate is at a temperature $t_{if} > t_s$. In the absence of gas, the interface temperature is the vapor saturation temperature at the pressure of the condenser.

The presence of noncondensable gas lowers the vapor partial pressure and hence the saturation temperature of the vapor in equilibrium with the condensate. Further, vapor movement toward the cooled surface implies similar bulk motion of the gas. At the condensing interface, vapor condenses at temperature t_{if} and is then swept out of the system as a liquid. The gas concentration rises to

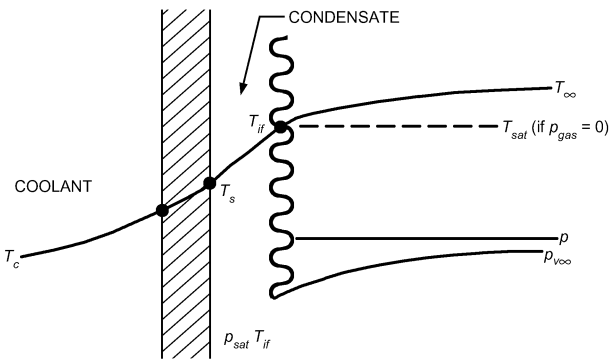

Fig. 7 Origin of Noncondensable Resistance

ultimately diffuse away from the cooled surface at the same rate as it is convected toward the surface (Figure 7). If gas (mole fraction) concentration is Y_g and total pressure of the system is p, the partial pressure of the bulk gas is

$$p_{g\infty} = Y_{g\infty}p \tag{4}$$

The partial pressure of the bulk vapor is

$$p_{v\infty} = (1 - Y_{g\infty})p = Y_{g\infty}p \tag{5}$$

As opposing fluxes of convection and diffusion of the gas increase, the partial pressure of gas at the condensing interface is $p_{gif} > p_{g\infty}$. By Dalton's law, assuming isobaric condition,

$$p_{gif} + p_{vif} = p \tag{6}$$

Hence, $p_{vif} < p_{v\infty}$.

Sparrow et al. (1967) noted that thermodynamic equilibrium exists at the interface, except in the case of very low pressures or liquid metal condensation, so that

$$p_{vif} = p_{sat}(t_{if}) \tag{7}$$

where $p_{sat}(t)$ is the saturation pressure of vapor at temperature t. The available Δt for condensation across the condensate film is reduced from $(t_\infty - t_s)$ to $(t_{if} - t_s)$, where t_∞ is the bulk temperature of the con-

densing vapor/gas mixture, caused by the additional noncondensable resistance.

The equations in Table 3 are still valid for condensate resistance, but interface temperature t_{if} must be found. The noncondensable resistance, which accounts for the temperature difference $(t_\infty - t_{if})$, depends on the heat flux (through the convecting flow to the interface) and the diffusion of gas away from the interface.

In simple cases, Rose (1969), Sparrow and Lin (1964), and Sparrow et al. (1967) found solutions to the combined energy, diffusion, and momentum problem of noncondensables, but they are cumbersome.

A general method given by Colburn and Hougen (1934) can be used over a wide range if correct expressions are provided for the rate equations; add the contributions of sensible heat transport through the noncondensable gas film and latent heat transport via condensation:

$$h_g(t_\infty - t_{if}) + K_D M_v h_{fg}(p_{v\infty} - p_{vif}) = h(t_{if} - t_s) = U(t_{if} - t_c) \tag{8}$$

where h is from the appropriate equation in Table 3.

The value of the heat transfer coefficient for stagnant gas depends on the geometry and flow conditions. For flow parallel to a condenser tube, for example,

$$j = \left[\frac{h_g}{(c_p)_g G}\right]\left[\frac{(c_p)_g \mu_{gv}}{K_{Dg}}\right]^{2/3} \tag{9}$$

where j is a known function of $\mathrm{Re} = GD/\mu_{gv}$. The mass transfer coefficient K_D is

$$\frac{K_D}{M_m}\left[\frac{p_{g\infty} - p_{gif}}{\ln(p_{g\infty}/p_{gif})}\right]\left(\frac{\mu_{gv}}{\rho_g D}\right)^{2/3} = j \tag{10}$$

The calculation method requires substitution of Equation (10) into Equation (8). For a given flow condition, G, Re, j, M_m, $\rho_{g\infty}$, h_g, and h (or U) are known. Assume values of t_{if}; calculate $p_{sat}(t_{if}) = p_{vif}$ and hence p_{gif}. If t_s is not known, use the overall coefficient U to the coolant and t_c in place of h and t_s in Equation (8). For either case, at each location in the condenser, iterate Equation (8) until it balances, giving the condensing interface temperature and, hence, the thermal load to that point (Colburn 1951; Colburn and Hougen 1934). For more detail, refer to Chapter 10 in Collier and Thome (1996).

Other Impurities

Vapor entering the condenser often contains a small percentage of impurities such as oil. Oil forms a film on the condensing surfaces, creating additional resistance to heat transfer. Some allowance should be made for this, especially in the absence of an oil separator or when the discharge line from the compressor to the condenser is short.

PRESSURE DROP

Total pressure drop for two-phase flow in tubes consists of friction, change in momentum, and gravitational components:

$$\left(\frac{dp}{dz}\right)_{total} = \left(\frac{dp}{dz}\right)_{static} + \left(\frac{dp}{dz}\right)_{mom} + \left(\frac{dp}{dz}\right)_{fric} \tag{11a}$$

The momentum pressure gradient accounts for the acceleration of the flow, usually caused by evaporation of liquid or condensation of vapor. In this case,

$$\left(\frac{dp}{dz}\right)_{mom} = G^3\left\{\left[\frac{(1-x)^2}{\rho_l(1-\varepsilon_v)} + \frac{x^2}{\rho_v \varepsilon_v}\right]_2 - \left[\frac{(1-x)^2}{\rho_l(1-\varepsilon_v)} + \frac{x^2}{\rho_v \varepsilon_v}\right]_1\right\} \tag{11b}$$

where G is total mass velocity, and subscripts 1 and 2 represent two different locations along the flow. An empirical model for the void fraction with good accuracy is presented by Steiner (1993), based on the (dimensional) correlation of Rouhani and Axelsson (1970).

$$\varepsilon_v = \frac{x}{\rho_v}\left\{[1 + 0.12(1-x)]\left(\frac{x}{\rho_v} + \frac{1-x}{\rho_l}\right) + \left[\frac{1.18(1-x)[g\sigma(\rho_l - \rho_v)]^{0.25}}{G^2 \rho_l^{0.5}}\right]\right\}^{-1} \tag{11c}$$

A generalized expression for ε_v was suggested by Butterworth (1975):

$$\varepsilon_v = \left[1 + A_l\left(\frac{1-x}{x}\right)^{q_l}\left(\frac{\rho_v}{\rho_l}\right)^{r_l}\left(\frac{\mu_l}{\mu_v}\right)^{S_l}\right]^{-1} \tag{11d}$$

This generalized form represents the models of several researchers; constants and exponents needed for each model are given in Table 4.

The homogeneous model provides a simple method for computing the acceleration and gravitational components of pressure drop. It assumes that flow can be characterized by average fluid properties and that the velocities of liquid and vapor phases are equal (Collier and Thome 1996; Wallis 1969). The following discussion of several empirical correlations for computing frictional pressure drop in two-phase internal flow is based on Ould Didi et al. (2002).

Friedel Correlation

A common strategy in both two-phase heat transfer and pressure drop modeling is to begin with a single-phase model and determine an appropriate **two-phase multiplier** to correct for the enhanced energy and momentum transfer in two-phase flow. The Friedel (1979) correlation follows this strategy:

$$\frac{dp}{dz} = \left(\frac{dp}{dz}\right)_l \Phi_{lo}^2 \tag{12a}$$

In this case,

$$\left(\frac{dp}{dz}\right)_l = 4f_l \frac{[G_{tot}(1-x)]^2}{2\rho_l D} \tag{12b}$$

with

$$f = \frac{0.079}{\mathrm{Re}^{0.25}} \tag{12c}$$

Table 4 Constants in Equation (11d) for Different Void Fraction Correlations

Model	A_l	q_l	r_l	S_l
Homogeneous (Collier 1972)	1.0	1.0	1.0	0
Lockhart and Martinelli (1949)	0.28	0.64	0.36	0.07
Baroczy (1963)	1.0	0.74	0.65	0.13
Thom (1964)	1.0	1.0	0.89	0.18
Zivi (1964)	1.0	1.0	0.67	0
Turner and Wallis (1965)	1.0	0.72	0.40	0.08

and

$$\mathrm{Re} = \frac{G_{tot} D}{\mu} \tag{12d}$$

with $\mu = \mu_l$ used to calculate f_l for use in Equation (12b). The two-phase multiplier Φ_{lo}^2 is determined by

$$\Phi_{lo}^2 = E + \frac{3.24FH}{\mathrm{Fr}_h^{0.045}\mathrm{We}_l^{0.035}} \tag{12e}$$

where

$$\mathrm{Fr}_h = \frac{G_{tot}^2}{gD\rho_h^2} \tag{12f}$$

$$E = (1-x)^2 + x^2\left(\frac{\rho_l}{\rho_v}\right)\left(\frac{f_v}{f_l}\right) \tag{12g}$$

$$F = x^{0.78}(1-x)^{0.224} \tag{12h}$$

$$H = \left(\frac{\rho_l}{\rho_v}\right)^{0.91}\left(\frac{\mu_v}{\mu_l}\right)^{0.19}\left(1-\frac{\mu_v}{\mu_l}\right)^{0.7} \tag{12i}$$

$$\mathrm{We}_l = \frac{G_{tot}^2 D}{\sigma_t \rho_h} \tag{12j}$$

Note that friction factors in Equation (12g) are calculated from Equations (12c) and (12d) using the vapor and liquid fluid properties, respectively. The homogeneous density ρ_h is given by

$$\rho_h = \left(\frac{x}{\rho_v} + \frac{1-x}{\rho_l}\right)^{-1} \tag{12k}$$

This method is generally recommended when the viscosity ratio μ_l/μ_v is less than 1000.

Lockhart and Martinelli Correlation

One of the earliest two-phase pressure drop correlations was proposed by Martinelli and Nelson (1948) and rendered more useful by Lockhart and Martinelli (1949). A relatively straightforward implementation of this model requires that Re_l be calculated first, based on Equation (12d) and liquid properties. If $\mathrm{Re}_l > 4000$,

$$\frac{dp}{dz} = \Phi_{ltt}^2\left(\frac{dp}{dz}\right)_l \tag{13a}$$

where

$$\Phi_{ltt}^2 = 1 + \frac{C}{X_{tt}} + \frac{1}{X_{tt}^2} \tag{13b}$$

and $(dp/dz)_l$ is calculated using Equation (12b).

If $\mathrm{Re}_l < 4000$,

$$\frac{dp}{dz} = \Phi_{Vtt}^2\left(\frac{dp}{dz}\right)_v \tag{13c}$$

where

$$\Phi_{Vtt}^2 = 1 + CX_{tt} + X_{tt}^2 \tag{13d}$$

In both cases,

$$X_{tt} = \left(\frac{1-x}{x}\right)^{0.9}\left(\frac{\rho_v}{\rho_l}\right)^{0.5}\left(\frac{\mu_l}{\mu_v}\right)^{0.1} \tag{13e}$$

and $C = 20$ for most cases of interest in internal flow in HVAC&R systems.

Grönnerud Correlation

Much of the two-phase pressure drop modeling has been based on adiabatic air/water data. To address this, Grönnerud (1979) developed a correlation based on refrigerant flow data, also using a two-phase multiplier:

$$\frac{dp}{dz} = \Phi_{gd}\left(\frac{dp}{dz}\right)_l \tag{14a}$$

with

$$\Phi_{gd} = 1 + \left(\frac{dp}{dz}\right)_{\mathrm{Fr}}\left[\frac{(\rho_l/\rho_v)}{(\mu_l/\mu_v)^{0.25}} - 1\right] \tag{14b}$$

The liquid-only pressure gradient in Equation (14a) is calculated as before, using Equation (12b) with $x = 0$ and

$$\left(\frac{dp}{dz}\right)_{\mathrm{Fr}} = f_{\mathrm{Fr}}\left[x + 4\left(x^{1.8} - x^{10} f_{\mathrm{Fr}}^{0.5}\right)\right] \tag{14c}$$

The friction factor f_{Fr} in this method depends on the liquid Froude number, defined by

$$\mathrm{Fr}_l = \frac{G_{tot}^2}{gD\rho_l^2} \tag{14d}$$

If Fr_l is greater than or equal to 1, $f_{\mathrm{Fr}} = 1.0$. If $\mathrm{Fr}_l < 1$,

$$f_{\mathrm{Fr}} = \mathrm{Fr}_l^{0.3} + 0.0055\left[\ln\left(\frac{1}{\mathrm{Fr}_l}\right)\right]^2 \tag{14e}$$

Müller-Steinhagen and Heck Correlation

A simple, purely empirical correlation was proposed by Müller-Steinhagen and Heck (1986):

$$\frac{dp}{dz} = \Lambda(1-x)^{1/3} + \left(\frac{dp}{dz}\right)_{vo} x^3 \tag{15a}$$

where

$$\Lambda = \left(\frac{dp}{dz}\right)_{lo} + 2\left[\left(\frac{dp}{dz}\right)_{vo} - \left(\frac{dp}{dz}\right)_{lo}\right]x \tag{15b}$$

and

$$\left(\frac{dp}{dz}\right)_{lo} = f_l \frac{2G_{tot}^2}{D\rho_l} \tag{15c}$$

$$\left(\frac{dp}{dz}\right)_{vo} = f_v \frac{2G_{tot}^2}{D\rho_v} \tag{15d}$$

where friction factors in Equations (15c) and (15d) are again calculated from Equations (12c) and (12d) using the liquid and vapor properties, respectively.

The general nature of annular vapor/liquid flow in vertical pipes is indicated in Figure 8 (Wallis 1970), which plots the effective vapor friction factor versus the liquid fraction $(1 - \varepsilon_v)$, where ε_v is the vapor void fraction as defined by Equations (11c) or (11d).

The effective vapor friction factor in Figure 8 is defined as

$$f_{eff} = \left[\frac{\varepsilon_v^{2.5} D}{2\rho_v \left(\frac{4Q_v}{\pi D^2}\right)^2}\right]\left(\frac{dp}{dz}\right) \quad (16a)$$

where D is the pipe diameter, ρ_v is gas density, and Q_v is volumetric flow rate. The friction factor of vapor flowing by itself in the pipe (presumed smooth) is denoted by f_v. Wallis' analysis of the flow occurrences is based on interfacial friction between the gas and liquid. The wavy film corresponds to a conduit with roughness height of about four times the liquid film thickness. Thus, the pressure drop relation for vertical flow is

$$\frac{dp}{dz} = 0.01\left(\frac{\rho_v}{D^5}\right)\left(\frac{4Q_v}{\pi}\right)^2\left(\frac{1+75(1-\varepsilon_v)}{\varepsilon_v^{2.5}}\right) \quad (16b)$$

This corresponds to the Martinelli-type analysis with

$$f_{two\text{-}phase} = \Phi_v^2 f_v \quad (16c)$$

when

$$\Phi_v^2 = \frac{1+75(1-\varepsilon_v)}{\varepsilon_v} \quad (16d)$$

The friction factor f_v (of the vapor alone) is taken as 0.02, an appropriate turbulent flow value. This calculation can be modified for more detailed consideration of factors such as Reynolds number variation in friction, gas compressibility, and entrainment (Wallis 1970).

Recommendations

Although many references recommend the Lockhart and Martinelli (1949) correlation, recent reviews of pressure drop correlations found other methods to be more accurate. Tribbe and Müller-Steinhagen (2000) found that the Müller-Steinhagen and Heck (1986) correlation worked quite well for a database of horizontal flows that included air/water, air/oil, steam, and several refrigerants. Ould Didi et al. (2002) also found that this method offered accuracies nearly as good or better than several other models; the Friedel (1979) and Grönnerud (1979) correlations also performed favorably. Note, however, that mean deviations of as much as 30% are common using these correlations; calculations for individual flow conditions can easily deviate 50% or more from measured pressure drops, so use these models as approximations only.

Evaporators and condensers often have valves, tees, bends, and other fittings that contribute to the overall pressure drop of the heat exchanger. Collier and Thome (1996) summarize methods predicting the two-phase pressure drop in these fittings.

Pressure Drop in Plate Heat Exchangers

For a description of plate heat exchanger geometry, see the Plate Heat Exchangers section of Chapter 4.

Ayub (2003) presented simple correlations for Fanning friction factor based on design and field data collected over a decade on ammonia and R-22 direct-expansion and flooded evaporators in North America. The goal was to formulate equations that could be readily used by a design and field engineer without reference to complicated two-phase models. Correlations within the plates are formulated as if the entire flow were saturated vapor. The correlation is accordingly adjusted for the chevron angle, and thus generalized for application to any type of commercially available plate, with a statistical error of ±10%:

$$f = (n/\mathrm{Re}^m)(-1.89 + 6.56R - 3.69R^2) \quad (17)$$

for $30 \le \beta \le 65$ where $R = (30/\beta)$, and β is the chevron angle in degrees. The values of m and n depend on Re.

m	*n*	Re
0.137	2.99	<4000
0.172	2.99	4000 < Re < 8000
0.161	3.15	8000 < Re < 16,000
0.195	2.99	>16,000

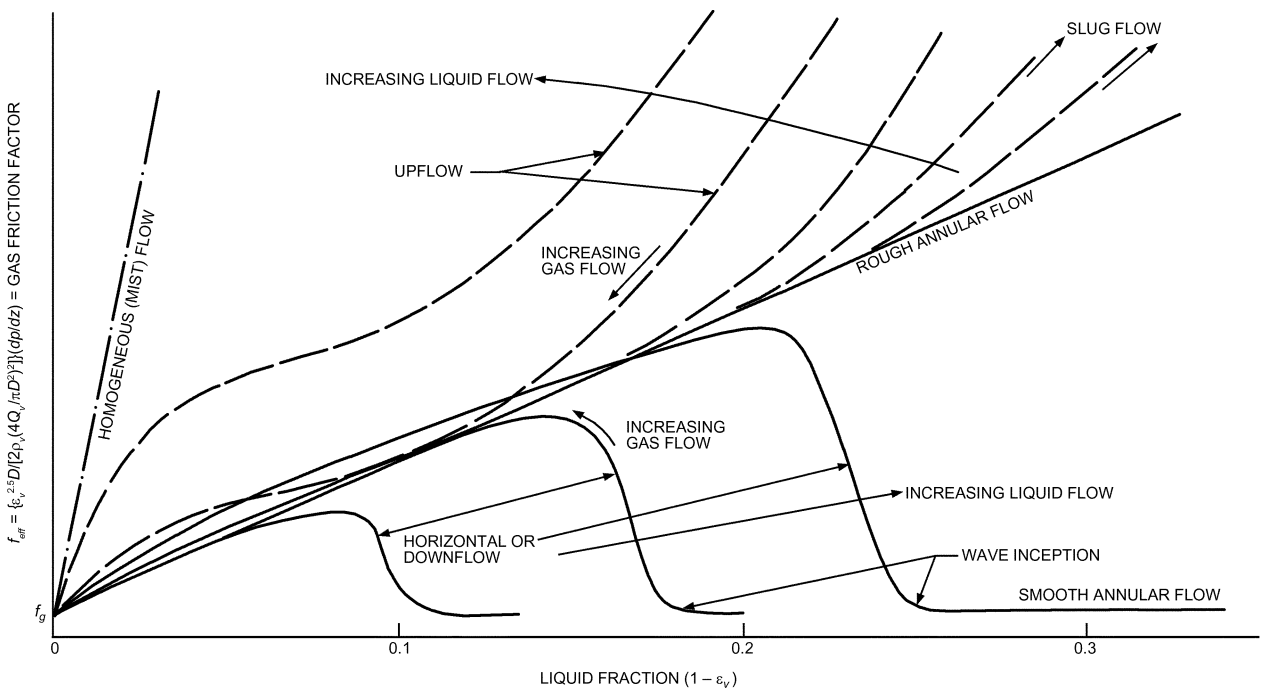

Fig. 8 Qualitative Pressure Drop Characteristics of Two-Phase Flow Regime
(Wallis 1970)

Pressure drop within the port holes is correlated as follows, treating the entire flow as saturated vapor:

$$\Delta p_{port} = 0.0076 \rho V^2/2g \quad (18)$$

This equation accounts for pressure drop in both inlet and outlet refrigerant ports and gives the pressure drop in units of lb/in^2 with input for ρ in lb/ft^3, V in ft/s, and g in ft/s^2.

ENHANCED SURFACES

Enhanced heat transfer surfaces are used in heat exchangers to improve performance and decrease cost. Condensing heat transfer is often enhanced with circular fins attached to the external surfaces of tubes to increase the heat transfer area. Other enhancement methods (e.g., porous coatings, integral fins, reentrant cavities) are used to augment boiling heat transfer on external surfaces of evaporator tubes. Webb (1981) surveyed external boiling surfaces and compared performances of several enhanced surfaces with performance of smooth tubes. For heat exchangers, the heat transfer coefficient for the refrigerant side is often smaller than the coefficient for the water side. Thus, enhancing the refrigerant-side surface can reduce the size of the heat exchanger and improve its performance.

Internal fins increase the heat transfer coefficients during evaporation or condensation in tubes. However, internal fins increase refrigerant pressure drop and reduce the heat transfer rate by decreasing the available temperature difference between hot and cold fluids. Designers should carefully determine the number of parallel refrigerant passes that give optimum loading for best overall heat transfer. For a review of internal enhancements for two-phase heat transfer, including the effects of oil, see Newell and Shah (2001).

For additional information on enhancement methods in two-phase flow, consult Bergles (1976, 1985), Thome (1990), and Webb (1994).

SYMBOLS

A = area, effective plate area
a = local acceleration
b = breadth of condensing surface. For vertical tube, $b = \pi d$; for horizontal tube, $b = 2L$; flow channel gap in flat plate heat exchanger.
Bo = boiling number
C = coefficient or constant
Co = convection number
c_p = specific heat at constant pressure
c_v = specific heat at constant volume
D = diameter
D_o = outside tube diameter
d = diameter; or prefix meaning differential
(dp/dz) = pressure gradient
$(dp/dz)_{fric}$ = frictional pressure gradient
$(dp/dz)_l$ = frictional pressure gradient, assuming that liquid alone is flowing in pipe
$(dp/dz)_{mom}$ = momentum pressure gradient
$(dp/dz)_v$ = frictional pressure gradient, assuming that gas (or vapor) alone is flowing in pipe
Fr = Froude number
f = friction factor for single-phase flow (Fanning)
G = mass velocity
g = gravitational acceleration
g_c = gravitational constant
Gr = Grashof number
h = heat transfer coefficient
h_f = single-phase liquid heat transfer coefficient
h_{fg} = latent heat of vaporization or of condensation
j = Colburn j-factor
k = thermal conductivity
K_D = mass transfer coefficient, dimensionless coefficient (Table 1)
L = length
L_p = plate length
M = mass; or molecular weight
m = general exponent
$\dot{m}$ = mass flow rate
M_m = mean molecular weight of vapor/gas mixture
M_v = molecular weight of condensing vapor
N = number of tubes in vertical tier
n = general exponent
Nu = Nusselt number
P = plate perimeter
p = pressure
p_c = critical thermodynamic pressure for coolant
p_g = partial pressure of noncondensable gas
Pr = Prandtl number
p_r = reduced pressure = p/p_c
p_v = partial pressure of vapor
Q_v = volumetric flow rate
q = heat transfer rate
r = radius
Ra = Rayleigh number
Re = Reynolds number
R_p = surface roughness, μm
t = temperature
U = overall heat transfer coefficient
V = linear velocity
We = Weber number
x = quality (i.e., mass fraction of vapor); or distance in dt/dx
X_{tt} = Martinelli parameter
x, y, z = lengths along principal coordinate axes
Y_g = mole fraction of noncondensable gas
Y_v = mole fraction of vapor

Greek

α = thermal diffusivity = $k/\rho c_p$
β = coefficient of thermal expansion, chevron angle
Γ = mass rate of flow of condensate per unit of breadth (see section on Condensing)
Δ = difference between values
ε = roughness of interface
ε_v = vapor void fraction
θ = contact angle
μ = absolute (dynamic) viscosity
μ_l = dynamic viscosity of saturated liquid
μ_v = dynamic viscosity of saturated vapor
ν = kinematic viscosity
ρ = density
ρ_l = density of saturated liquid
ρ_v = density of saturated vapor phase
σ = surface tension
Φ = two-phase multiplier
ϕ = fin efficiency

Subscripts and Superscripts

a = exponent in Equation (1)
b = bubble
c = critical, cold (fluid), characteristic, coolant
e = equivalent
eff = effective
f = film or fin
$fric$ = friction
g = noncondensable gas
gv = noncondensable gas and vapor mixture
h = horizontal, hot (fluid), hydraulic
i = inlet or inside
if = interface
l = liquid
m = mean
mac = convective mechanism
max = maximum
mic = nucleation mechanism
min = minimum
mom = momentum
ncb = nucleate boiling
o = outside, outlet, overall, reference
r = root (fin) or reduced pressure
s = surface or secondary heat transfer surface
sat = saturation
t = temperature or terminal temperature of tip (fin)
tot = total
v = vapor or vertical
w = wall
∞ = bulk or far-field
$*$ = reference

REFERENCES

Anderson, W., D.G. Rich, and D.F. Geary. 1966. Evaporation of Refrigerant 22 in a horizontal 3/4-in. OD tube. *ASHRAE Transactions* 72(1):28.

Ayub, Z.H. 2003. Plate heat exchanger literature survey and new heat transfer and pressure drop correlations for refrigerant evaporators. *Heat Transfer Engineering* 24(5):3-16.

Barnea, D. and Y. Taitel. 1986. Flow pattern transition in two-phase gas-liquid flows. In *Encyclopedia of Fluid Mechanics*, vol. 3. Gulf Publishing, Houston.

Baroczy, C.J. 1963. Correlation of liquid fraction in two-phase flow with application to liquid metals. North American Aviation *Report* SR-8171, El Segundo, CA.

Baskin, E. 1991. Applicability of plate heat exchangers in heat pumps. *ASHRAE Transactions* 97(2):305-308.

Beatty, K.O. and D.L. Katz. 1948. Condensation of vapors on outside of finned tubes. *Chemical Engineering Progress* 44(1):55.

Bennett, D.L. and J.C. Chen. 1980. Forced convective boiling in vertical tubes for saturated pure components and binary mixtures. *AIChE Journal* 26(3):454-461.

Berenson, P.J. 1961. Film boiling heat transfer from a horizontal surface. *ASME Journal of Heat Transfer* 85:351.

Berenson, P.J. 1962. Experiments on pool boiling heat transfer. *International Journal of Heat and Mass Transfer* 5:985.

Bergles, A.E. 1976. Survey and augmentation of two-phase heat transfer. *ASHRAE Transactions* 82(1):891-905.

Bergles, A.E. 1985. Techniques to augment heat transfer. In *Handbook of heat transfer application*, 2nd ed. McGraw-Hill, New York.

Bergles, A.E. and W.M. Rohsenow. 1964. The determination of forced convection surface-boiling heat transfer. *ASME Journal of Heat Transfer*, Series C, 86(August):365.

Borishansky, W. and A. Kosyrev. 1966. Generalization of experimental data for the heat transfer coefficient in nucleate boiling. *ASHRAE Journal* (May):74.

Borishansky, V.M., I.I. Novikov, and S.S. Kutateladze. 1962. Use of thermodynamic similarity in generalizing experimental data on heat transfer. *Proceedings of the International Heat Transfer Conference*.

Breber, G., J.W. Palen, and J. Taborek. 1980. Prediction of the horizontal tubeside condensation of pure components using flow regime criteria. *ASME Journal of Heat Transfer* 102(3):471-476.

Bromley, L.A. 1950. Heat transfer in stable film boiling. *Chemical Engineering Progress* (46):221.

Brusstar, M.J. and H. Merte, Jr. 1997. Effects of heater surface orientation on the critical heat flux—II. A model for pool and forced convection subcooled boiling. *International Journal of Heat and Mass Transfer* 40(17):4021-4030.

Butterworth, D. 1975. A comparison of some void-fraction relationships for co-current gas-liquid flow. *International Journal of Multiphase Flow* 1:845-850.

Carey, V.P. 1992. *Liquid-vapor phase change phenomena: An introduction to the thermophysics of vaporization and condensation processes in heat transfer equipment*. Hemisphere Publishing, Washington, D.C.

Cavallini, A. and R. Zecchin, 1974. A dimensionless correlation for heat transfer in forced convection condensation. *Proceedings of the 5th International Heat Transfer Conference* 3:309-313.

Cavallini, A., G. Censi, D. Del Col, L. Doretti, G.A. Longo, and L. Rosetto. 2002. In-tube condensation of halogenated refrigerants. *ASHRAE Transactions* 108(1):146-161.

Chaddock, J.B. and J.A. Noerager. 1966. Evaporation of Refrigerant 12 in a horizontal tube with constant wall heat flux. *ASHRAE Transactions* 72(1):90.

Chen, J.C. 1963. A correlation for boiling heat transfer to saturated fluids on convective flow. ASME *Paper* 63-HT-34. American Society of Mechanical Engineers, New York.

Chen, J.C. 2003. Surface contact—Its significance for multiphase heat transfer: Diverse examples. *Journal of Heat Transfer* 125:549-566.

Colburn, A.P. 1951. Problems in design and research on condensers of vapours and vapour mixtures. *Proceedings of the Institute of Mechanical Engineers*, London, vol. 164, p. 448.

Colburn, A.P. and O.A. Hougen. 1934. Design of cooler condensers for mixtures of vapors with noncondensing gases. *Industrial and Engineering Chemistry* 26 (November):1178.

Coleman, J.W. and S. Garimella. 1999. Characterization of two-phase flow patterns in small-diameter round and rectangular tubes. *International Journal of Heat and Mass Transfer* 42:2869-2881.

Collier, J.G. 1972. *Convective boiling and condensation*. McGraw-Hill.

Collier, J.G. and J.R. Thome. 1996. *Convective boiling and condensation*, 3rd ed. Oxford University Press.

Cooper, M.G. 1984. Heat flow rates in saturated nucleate pool boiling—A wide-ranging examination using reduced properties. *Advances in Heat Transfer* 16:157-239.

Danilova, G. 1965. Influence of pressure and temperature on heat exchange in the boiling of halogenated hydrocarbons. *Kholodilnaya Teknika* 2. English abstract, *Modern Refrigeration* (December).

Dhir, V.K. and S.P. Liaw. 1989. Framework for a unified model for nucleate and transition pool boiling. *Journal of Heat Transfer* 111:739-745.

Dhir, V. K. and J. Lienhard. 1971. Laminar film condensation on plan and axisymmetric bodies in non-uniform gravity. *Journal of Heat Transfer* 91:97-100.

Dobson, M.K. and J.C. Chato. 1998. Condensation in smooth horizontal tubes. *Journal of Heat Transfer* 120:193-213.

Dougherty, R.L. and H.J. Sauer, Jr. 1974. Nucleate pool boiling of refrigerant-oil mixtures from tubes. *ASHRAE Transactions* 80(2):175.

Eckels, S.J., T.M. Doer, and M.B. Pate. 1994. In-tube heat transfer and pressure drop of R-134a and ester lubricant mixtures in a smooth tube and a micro-fin tube, part 1: Evaporation. *ASHRAE Transactions* 100(2): 265-282.

El Hajal, J., J.R. Thome, and A. Cavallini. 2003. Condensation in horizontal tubes, part 1: Two-phase flow pattern map. *International Journal of Heat and Mass Transfer* 46(18):3349-3363.

Farber, E.A. and R.L. Scorah. 1948. Heat transfer to water boiling under pressure. *ASME Transactions* (May):373.

Frederking, T.H.K. and J.A. Clark. 1962. Natural convection film boiling on a sphere. In *Advances in cryogenic engineering*, K.D. Timmerhouse, ed. Plenum Press, New York.

Friedel, L. 1979. Improved friction pressure drop correlations for horizontal and vertical two-phase pipe flow. European Two-Phase Flow Group Meeting, Paper E2, Ispra, Italy.

Fujii, T. 1995. Enhancement to condensing heat transfer—New developments. *Journal of Enhanced Heat Transfer* 2:127-138.

Furse, F.G. 1965. Heat transfer to Refrigerants 11 and 12 boiling over a horizontal copper surface. *ASHRAE Transactions* 71(1):231.

Gorenflo, D. 1993. *Pool boiling*. VDI-Heat Atlas. VDI-Verlag, Düsseldorf.

Gouse, S.W., Jr. and K.G. Coumou. 1965. Heat transfer and fluid flow inside a horizontal tube evaporator, phase I. *ASHRAE Transactions* 71(2):152.

Green, G.H. and F.G. Furse. 1963. Effect of oil on heat transfer from a horizontal tube to boiling Refrigerant 12-oil mixtures. *ASHRAE Journal* (October):63.

Grober, H., S. Erk, and U. Grigull. 1961. *Fundamentals of heat transfer*. McGraw-Hill, New York.

Grönnerud, R. 1979. Investigation of liquid hold-up, flow resistance and heat transfer in circulation type evaporators, part IV: Two-phase flow resistance in boiling refrigerants. Annexe 1972-1, *Bulletin de l'Institut du Froid*.

Guerrieri, S.A. and R.D. Talty. 1956. A study of heat transfer to organic liquids in single tube boilers. *Chemical Engineering Progress Symposium Series* 52(18):69.

Gungor, K.E. and R.H.S. Winterton. 1986. A general correlation for flow boiling in tubes and annuli. *International Journal of Heat and Mass Transfer* 29:351-358.

Gungor, K.E. and R.H.S. Winterton. 1987. Simplified general correlation for saturated flow boiling and comparison of correlations with data. *Chemical Engineering Research and Design* 65:148-156.

Hall, D.D. and I. Mudawar. 2000a. Critical heat flux (CHF) for water flow in tubes—I. Compilation and assessment of world CHF data. *International Journal of Heat and Mass Transfer* 43(14):2573-2604.

Hall, D.D. and I. Mudawar. 2000b. Critical heat flux (CHF) for water flow in tubes—II: Subcooled CHF correlations. *International Journal of Heat and Mass Transfer* 43(14):2605-2640.

Haramura, Y. and Y. Katto. 1983. A new hydrodynamic model of critical heat flux, applicable widely to both pool and forced convection boiling on submerged bodies in saturated liquids. *International Journal of Heat and Mass Transfer* 26:389-399.

Hesselgreaves, J.E. 1990. The impact of compact heat exchangers on refrigeration technology and CFC replacement. *Proceedings of the 1990 USNC/IIR-Purdue Refrigeration Conference*, ASHRAE/Purdue CFC Conference, pp. 492-500.

Hetsroni, G., ed. 1986. *Handbook of multiphase systems*. Hemisphere Publishing, Washington D.C.

Howard, A.H. and I. Mudawar. 1999. Orientation effects on pool boiling critical heat flux (CHF) and modeling of CHF for near-vertical surfaces. *International Journal of Heat and Mass Transfer* 42:1665-1688.

Hughmark, G.A. 1962. A statistical analysis of nucleate pool boiling data. *International Journal of Heat and Mass Transfer* 5:667.

Incropera, F.P. and D.P. DeWitt. 2002. *Fundamentals of heat and mass transfer*, 5th ed. John Wiley & Sons, New York.

Isrealachvili, J.N. 1991. *Intermolecular surface forces*. Academic Press, New York.

Jakob, M. 1949, 1957. *Heat transfer*, vols. I and II. John Wiley & Sons, New York.

Jonsson, I. 1985. Plate heat exchangers as evaporators and condensers for refrigerants. *Australian Refrigeration, Air Conditioning and Heating* 39(9):30-31, 33-35.

Kandlikar, S.G., ed. 1999. *Handbook of phase change: Boiling and condensation*. Taylor and Francis, Philadelphia.

Kandlikar, S.G. 2001. A theoretical model to predict pool boiling CHF incorporating effects of contact angle and orientation. *Journal of Heat Transfer* 123:1071-1079.

Kattan, N., J.R. Thome, and D. Favrat. 1998a. Flow boiling in horizontal tubes, part 1: Development of diabatic two-phase flow pattern map. *Journal of Heat Transfer* 120(1):140-147.

Kattan, N., J.R. Thome, and D. Favrat. 1998b. Flow boiling in horizontal tubes, part 3: Development of new heat transfer model based on flow patterns. *Journal of Heat Transfer* 120(1):156-165.

Kumar, H. 1984. The plate heat exchanger: Construction and design. *Institute of Chemical Engineering Symposium Series* 86:1275-1288.

Kutateladze, S.S. 1951. A hydrodynamic theory of changes in the boiling process under free convection. Izvestia Akademii Nauk, USSR, *Otdelenie Tekhnicheski Nauk* 4:529.

Kutateladze, S.S. 1963. *Fundamentals of heat transfer*. E. Arnold Press, London.

Lienhard, J.H. and V.E. Schrock. 1963. The effect of pressure, geometry and the equation of state upon peak and minimum boiling heat flux. *ASME Journal of Heat Transfer* 85:261.

Lienhard, J.H. and P.T.Y. Wong. 1964. The dominant unstable wavelength and minimum heat flux during film boiling on a horizontal cylinder. *Journal of Heat Transfer* 86:220-226.

Lockhart, R.W. and R.C. Martinelli. 1949. Proposed correlation of data for isothermal two-phase, two-component flow in pipes. *Chemical Engineering Progress* 45(1):39-48.

Mandhane, J.M., G.A. Gregory, and K. Aziz. 1974. A flow pattern map for gas-liquid flow in horizontal pipes. *International Journal of Multiphase Flow* 1:537-553.

Martinelli, R.C. and D.B. Nelson. 1948. Prediction of pressure drops during forced circulation boiling of water. *ASME Transactions* 70:695.

McAdams, W.H. 1954. *Heat transmission*, 3rd ed. McGraw-Hill, New York.

McGillis, W.R. and V.P. Carey. 1996. On the role of the Marangoni effects on the critical heat flux for pool boiling of binary mixture. *Journal of Heat Transfer* 118(1):103-109.

Müller-Steinhagen, H. and K. Heck. 1986. A simple friction pressure drop correlation for two-phase flow in pipes. *Chemical Engineering Progress* 20:297-308.

Newell, T.A. and R.K. Shah. 2001. An assessment of refrigerant heat transfer, pressure drop, and void fraction effects in microfin tubes. *International Journal of HVAC&R Research* 7(2):125-153.

Nukiyama, S. 1934. The maximum and minimum values of heat transmitted from metal to boiling water under atmospheric pressure. *Journal of the Japanese Society of Mechanical Engineers* 37:367.

Nusselt, W. 1916. Die Oberflächenkondensation des Wasserdampfes. *Zeitung Verein Deutscher Ingenieure* 60:541.

Othmer, D.F. 1929. The condensation of steam. *Industrial and Engineering Chemistry* 21(June):576.

Ould Didi, M.B., N. Kattan and J.R. Thome. 2002. Prediction of two-phase pressure gradients of refrigerants in horizontal tubes. *International Journal of Refrigeration* 25:935-947.

Palen, J. and Z.H. Yang. 2001. Reflux condensation flooding prediction: A review of current status. *Transactions of the Institute of Chemical Engineers* 79(A):463-469.

Panchal, C.B. 1985. Condensation heat transfer in plate heat exchangers. *Two-Phase Heat Exchanger Symposium*, HTD vol. 44, pp. 45-52. American Society of Mechanical Engineers, New York.

Panchal, C.B. 1990. Experimental investigation of condensation of steam in the presence of noncondensable gases using plate heat exchangers. Argonne National Laboratory *Report* CONF-900339-1.

Panchal, C.B. and D.L. Hillis. 1984. OTEC Performance tests of the Alfa-Laval plate heat exchanger as an ammonia evaporator. Argonne National Laboratory *Report* ANL-OTEC-PS-13.

Panchal, C.B., D.L. Hillis, and A. Thomas. 1983. Convective boiling of ammonia and Freon 22 in plate heat exchangers. Argonne National Laboratory *Report* CONF-830301-13.

Perry, J.H. 1950. *Chemical engineers handbook*, 3rd ed. McGraw-Hill, New York.

Pierre, B. 1964. Flow resistance with boiling refrigerant. *ASHRAE Journal* (September/October).

Reddy, R.P. and J.H. Lienhard. 1989. The peak heat flux in saturated ethanol-water mixtures. *Journal of Heat Transfer* 111:480-486.

Rohsenow, W.M. 1963. Boiling heat transfer. In *Modern developments in heat transfer*, W. Ibele, ed. Academic Press, New York.

Rohsenow, W.M. and P. Griffith. 1956. Correlation of maximum heat flux data for boiling of saturated liquids. *Chemical Engineering Progress Symposium Series* 52:47-49.

Rohsenow, W.M., J.P. Hartnett, and Y.I. Cho. 1998. *Handbook of heat transfer*, 3rd ed., pp. 1570-1571. McGraw-Hill.

Rose, J.W. 1969. Condensation of a vapour in the presence of a noncondensable gas. *International Journal of Heat and Mass Transfer* 12:233.

Rose, J.W. 1998. Condensation heat transfer fundamentals. *Transactions of the Institution of Chemical Engineers* 76(A):143-152.

Rouhani, Z. and E. Axelsson. 1970. Calculation of void volume fraction in the subcooled and quality boiling regions. *International Journal of Heat and Mass Transfer* 13:383-393.

Schlager, L.M., M.B. Pate, and A.E. Bergles. 1987. Evaporation and condensation of refrigerant-oil mixtures in a smooth tube and micro-fin tube. *ASHRAE Transactions* 93:293-316.

Sefiane, K. 2001. A new approach in the modeling of the critical heat flux and enhancement techniques. *AIChE Journal* 47(11):2402-2412.

Shah, M.M. 1979. A general correlation for heat transfer during film condensation inside pipes. *International Journal of Heat and Mass Transfer* 22:547-556.

Shah, M.M. 1982. A new correlation for saturated boiling heat transfer: Equations and further study. *ASHRAE Transactions* 88(1):185-196.

Sparrow, E.M. and S.H. Lin. 1964. Condensation in the presence of a non-condensable gas. *ASME Transactions, Journal of Heat Transfer* 86C: 430.

Sparrow, E.M., W.J. Minkowycz, and M. Saddy. 1967. Forced convection condensation in the presence of noncondensables and interfacial resistance. *International Journal of Heat and Mass Transfer* 10:1829.

Spedding, P.L. and D.R. Spence. 1993. Flow regimes in two-phase gas-liquid flow. *International Journal of Multiphase Flow* 19(2):245-280.

Starczewski, J. 1965. Generalized design of evaporation heat transfer to nucleate boiling liquids. *British Chemical Engineering* (August).

Steiner, D. 1993. *VDI-Wärmeatlas (VDI Heat Atlas)*. Verein Deutscher Ingenieure, VDI-Gesellschaft Verfahrenstechnik und Chemieingenieurwesen (GCV), Düsseldorf, Chapter Hbb.

Steiner, D. and J. Taborek. 1992. Flow boiling heat transfer in vertical tubes correlated by an asymptotic model. *Heat Transfer Engineering* 13(2): 43-69.

Stephan, K. 1963. Influence of oil on heat transfer of boiling Freon-12 and Freon-22. Eleventh International Congress of Refrigeration, IIR *Bulletin* 3.

Stephan, K. 1992. *Heat transfer in condensation and boiling*. Springer-Verlag, Berlin.

Stephan, K. and M. Abdelsalam. 1980. Heat transfer correlations for natural convection boiling. *International Journal of Heat and Mass Transfer* 23:73-87.

Syed, A. 1990. The use of plate heat exchangers as evaporators and condensers in process refrigeration. Symposium on Advanced Heat Exchanger Design. Institute of Chemical Engineers, Leeds, U.K.

Thom, J.R.S. 1964. Prediction of pressure drop during forced circulation boiling water. *International Journal of Heat and Mass Transfer* 7: 709-724.

Thome, J.R. 1990. *Enhanced boiling heat transfer*. Hemisphere (Taylor and Francis), New York.

Thome, J.R. 2001. Flow regime based modeling of two-phase heat transfer. *Multiphase Science and Technology* 13(3-4):131-160.

Thome, J.R. 2003. Update on the Kattan-Thome-Favrat flow boiling model and flow pattern map. Fifth International Conference on Boiling Heat Transfer, Montego Bay, Jamaica.

Thome, J.R. and A.W. Shock. 1984. Boiling of multicomponent liquid mixtures. In *Advances in heat transfer*, vol. 16, pp. 59-156. Academic Press, New York.

Thome, J.R., J. El Hajal, and A. Cavallini. 2003. Condensation in horizontal tubes, Part 2: New heat transfer model based on flow regimes. *International Journal of Heat and Mass Transfer* 46(18):3365-3387.

Thonon, B. 1995. Design method for plate evaporators and condensers. *1st International Conference on Process Intensification for the Chemical Industry, BHR Group Conference Series Publication* 18, pp. 37-47.

Thonon, B., R. Vidil, and C. Marvillet. 1995. Recent research and developments in plate heat exchangers. *Journal of Enhanced Heat Transfer* 2(12):149-155.

Tribbe, C. and H. Müller-Steinhagen. 2000. An evaluation of the performance of phenomenological models for predicting pressure gradient during gas-liquid flow in horizontal pipelines. *International Journal of Multiphase Flow* 26:1019-1036.

Tschernobyiski, I. and G. Ratiani. 1955. *Kholodilnaya Teknika* 32.

Turner, J.M. and G.B. Wallis. 1965. The separate-cylinders model of two-phase flow. *Report* NYO-3114-6. Thayer's School of Engineering, Dartmouth College, Hanover, NH.

Van Stralen, S.J. 1959. Heat transfer to boiling binary liquid mixtures. *British Chemical Engineering* 4(January):78.

Van Stralen, S.J. and R. Cole. 1979. *Boiling phenomena*, vol. 1. Hemisphere Publishing, Washington, D.C.

Wallis, G.B. 1969. *One-dimensional two-phase flow.* McGraw-Hill, New York.

Wallis, G.C. 1970. Annular two-phase flow, part I: A simple theory, part II: Additional effect. *ASME Transactions, Journal of Basic Engineering* 92D:59 and 73.

Webb, R.L. 1981. The evolution of enhanced surface geometrics for nucleate boiling. *Heat Transfer Engineering* 2(3-4):46-69.

Webb, J.R. 1994. *Enhanced boiling heat transfer*. John Wiley & Sons, New York.

Westwater, J.W. 1963. Things we don't know about boiling. In *Research in Heat Transfer*, J. Clark, ed. Pergamon Press, New York.

Worsoe-Schmidt, P. 1959. Some characteristics of flow-pattern and heat transfer of Freon-12 evaporating in horizontal tubes. *Ingenieren*, International edition, 3(3).

Yan, Y.-Y. and T.-F. Lin. 1999. Evaporation heat transfer and pressure drop of refrigerant R-134a in a plate heat exchanger. *Journal of Heat Transfer* 121(1):118-127.

Young, M. 1994. Plate heat exchangers as liquid cooling evaporators in ammonia refrigeration systems. *Proceedings of the IIAR 16th Annual Meeting*, St. Louis.

Zeurcher O., J.R. Thome, and D. Favrat. 1998. In-tube flow boiling of R-407C and R-407C/oil mixtures, part II: Plain tube results and predictions. *International Journal of HVAC&R Research* 4(4):373-399.

Zivi, S.M. 1964. Estimation of steady-state steam void-fraction by means of the principle of minimum entropy production. *Journal of Heat Transfer* 86:247-252.

Zuber, N. 1959. Hydrodynamic aspects of boiling heat transfer. U.S. Atomic Energy Commission, Technical Information Service, *Report* AECU 4439. Oak Ridge, TN.

Zuber, N., M. Tribus, and J.W. Westwater. 1962. The hydrodynamic crisis in pool boiling of saturated and subcooled liquids. *Proceedings of the International Heat Transfer Conference* 2:230, and discussion of the papers, vol. 6.